AD-A033 569 MARTIN MARIETTA LABS BALTIMORE MD F/G 20/4
SEPARATION OF THREE-DIMENSIONAL FLOW.(U)
AUG 76 K C WANG F49620-76-C-0004
UNCLASSIFIED MML-TR-76-54C NL

1 OF 1
AD-A
033 569

END
DATE
FILMED
1-26-77
NTIS

SEPARATION OF THREE-DIMENSIONAL FLOW

MARTIN MARIETTA LABORATORIES
BALTIMORE, MARYLAND

AUGUST 1976

MARTIN MARIETTA

Martin Marietta Laboratories

MML TR-76-54c

SEPARATION OF THREE-DIMENSIONAL FLOW

K. C. Wang

August 1976

Research sponsored by the Air Force Office of Scientific Research (AFSC), United States Air Force, under Contract F49620-76-C-0004.

Unclassified

SECURITY CLASSIFICATION OF THIS PAGE (When Data Entered)

REPORT DOCUMENTATION PAGE		READ INSTRUCTIONS BEFORE COMPLETING FORM
1. REPORT NUMBER MML TR 76-54c	2. GOVT ACCESSION NO.	3. RECIPIENT'S CATALOG NUMBER
4. TITLE (and Subtitle) Separation of Three-Dimensional Flow		5. TYPE OF REPORT & PERIOD COVERED Technical Report
		6. PERFORMING ORG. REPORT NUMBER MML TR-76-54c
7. AUTHOR(s) K. C. Wang		8. CONTRACT OR GRANT NUMBER(s) F49620-76-C-0004
9. PERFORMING ORGANIZATION NAME AND ADDRESS Martin Marietta Laboratories Martin Marietta Corporation 1450 South Rolling Road Baltimore, Maryland 21227		10. PROGRAM ELEMENT, PROJECT, TASK AREA & WORK UNIT NUMBERS
11. CONTROLLING OFFICE NAME AND ADDRESS		12. REPORT DATE August 1976
		13. NUMBER OF PAGES 80
14. MONITORING AGENCY NAME & ADDRESS(if different from Controlling Office)		15. SECURITY CLASS. (of this report) Unclassified
		15a. DECLASSIFICATION/DOWNGRADING SCHEDULE

16. DISTRIBUTION STATEMENT (of this Report)

Approved for public release; distribution unlimited.

17. DISTRIBUTION STATEMENT (of the abstract entered in Block 20, if different from Report)

18. SUPPLEMENTARY NOTES

19. KEY WORDS (Continue on reverse side if necessary and identify by block number)

Three-dimensional flow separation, open vs closed separations
Separation over inclined bodies
Separation over finite wings
Separation around corners

20. ABSTRACT (Continue on reverse side if necessary and identify by block number)

Separation patterns of three-dimensional flow are discussed here, partly on the basis of limited calculated results, but mostly on experimental observations and intuition. Generally the separation pattern is rather independent of whether the boundary layer is laminar or turbulent and whether the flow is incompressible or hypersonic. The difference is in degree, not character. Various three-dimensional separation criteria are reviewed and the open-vs-closed separation idea, particularly is presented,

DD FORM 1 JAN 73 1473 EDITION OF 1 NOV 65 IS OBSOLETE

Unclassified

SECURITY CLASSIFICATION OF THIS PAGE (When Data Entered)

in detail. The bulk of this work is divided into three parts, dealing with the separation over elongated inclined bodies, airplane wings at incidence, and around the corners between intersecting bodies.

SEPARATION OF THREE-DIMENSIONAL FLOW

K. C. Wang

MML TR 76-54c

August 1976

Research Sponsored by the Air Force of Scientific Research (AFSC), United States Air Force, under Contract F49620-76-C-0004.

Martin Marietta Corporation
Martin Marietta Laboratories
1450 South Rolling Road
Baltimore, Maryland 21227

This work was presented at the Viscous Flow Symposium at Lockheed-Georgia Company, Atlanta, Georgia, June 22-23, 1976.

CONTENTS

SUMMARY

Separation patterns of three-dimensional flow are discussed here, partly on the basis of limited calculated results, but mostly on experimental observations and intuition. Generally the separation pattern is rather independent of whether the boundary layer is laminar or turbulent and whether the flow is incompressible or hypersonic. The difference is in degree, not character. Various three-dimensional separation criteria are reviwed and the open-vs-closed separation idea, particularly is presented, in detail. The bulk of this work is divided into three parts, dealing with the separation over elongated inclined bodies, airplane wings at incidence, and around the corners between intersecting bodies.

I. INTRODUCTION

1.1 Preliminary Remarks

In recent years, boundary layer research has finally begun moving into the area of three-dimensional flows. Considerable progress has been achieved in our understanding of three-dimensional separation, experimentally and theoretically, although much more remains to be done.

In this work, after some brief remarks about two-dimensional spearation, we shall first discuss some general separation ideas for three-dimensional flow, in particular the idea of open separation vs. closed separation (Section 2). The rest of this work is then divided into three parts dealing with separation over bodies (Section 3), wings (Section 4) and in corners (Section 5). These three groups of problems are common in aerospace applications, and are also the most widely studied areas thus far. The basic ideas, of course, apply to similar cases of different physical interest as well.

The underlying approach is to illustrate three-dimensional separation of various specific examples, and hopefully to sort out some general characteristics from them. In the body-flow problem, separation patterns first determined by calculation are shown to have been confirmed by experiments. In the wing flow and the corner flow, calculated results are still lacking so our discussion relys on surface flow experiments and physical intuition. The experiments reported in the literature were originally made some time ago for different purposes; also, the flow speed involved varies from incompressible to hypersonic. This diversity of

experimental conditions does not cause any inconsistency in the present work because the separation patterns appear to be rather independent of the Mach number from all the evidence that has been examined. Compressibility, of course, influences many other flow phenomena such as shock waves and heat transfer.

Surveys of three-dimensional flow separation have previously been made by a number of authors, for example, Refs. 1-4. The scope of discussion in this work is influenced by the personal interest of the author, and the literature cited is not intended to be extensive. For some problems which have been repeatedly studied, it is difficult to determine who did what first.

Only steady flows are considered here and, in most cases, only primary separation is indicated. We shall make no effort to distinguish whether the separation is laminar or turbulent. The calculated separation patterns to be discussed are laminar cases, but many of the cited flow visualization experiments were made in turbulent flow. There are many differences between laminar and turbulent boundary layer flows, but the resulting separation patterns, to this author's knowledge, generally appear to be very similar. A laminar separation is usually more extended in area and depends on the Reynolds number, whereas a turbulent separation for what is otherwise the same flow is more confined and less dependent on the Reynolds number. The difference is a matter of degree, rather than character.

1.2 Two-Dimensional Separation

For two-dimensional flows, the criterion of separation[5-7] as first conceived by Prandtl is defined by

$$\left(\frac{\partial u}{\partial z}\right)_{z=0} = 0, \quad (1)$$

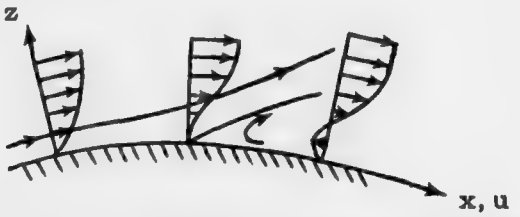

Fig. 1.1. Two-dimensional separation

which is mathematically precise and convenient to apply. Physically it states that the vanishing of skin friction marks the onset of separation. Associated with this idea of separation, there have been known a number of common notions or symptoms, each of which characterizes a certain aspect of the whole phenomenon. Some of them, individually or in combination, have become synonymous with separation and have even been taken as alternative definitions. In two-dimensional flow, it is interesting to note that these characteristics almost imply each other. They are listed below:

1. Singularity - separation is said to reflect mathematically a singularity of the boundary layer solution.
2. Reverse flow - separation is said to signify the onset of flow reversal.
3. Inaccessibility - separation determines a separated region which is inaccessible to the upstream flow.

4. Boundary layer thickening - Separation is marked by a rapid growth of the boundary layer thickness.
5. Breakdown of boundary layer assumptions - separation means that the basic boundary layer assumptions become invalid.
6. Computation difficulties - Convergence difficulty and increase of the number of iterations imply separation.

The question concerning us here is: Are these ideas still valid for three-dimensional separation? The answer seems to be some of these are, some are not, some need be modified and, for some, there is no answer yet. These points will become clear in the next section.

Another aspect of interest concerns the trend of separation. For a two-dimensional cylinder (say an elliptic cylinder, Fig. 1.2), a simple rule is that the separation point always moves forward as the incidence

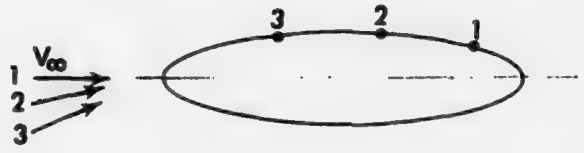

Fig. 1.2 Separation movement with incidence

increases. We would like to know: Is this trend also true for an ellipsoid of revolution at incidence?

In spite of early realization that three-dimensional separation requires new thinking, the influence of two-dimensional separation concepts

remains strong. Our knowledge of two-dimensional separation has really been a mixed blessing in our progress toward understanding of three-dimensional separation.

2. THREE-DIMENSIONAL SEPARATION

For separation in three dimensions, we first discuss the limiting streamlines and its singularities. Various three-dimensional separation criteria are reviewed next. Finally, the idea of open vs. closed separation is elaborated.

2.1. Limiting Streamlines and Singularities

The streamlines nearest to a body surface are known as the limiting streamlines. Study of the pattern of the limiting streamlines provides a good deal of insight about separation of steady flows. They are defined by

$$\frac{h_y\, dy}{h_x\, dx} = \frac{\cancel{v} + \left(\frac{\partial v}{\partial z}\right)_{z=0} z + \left(\frac{\partial^2 v}{\partial z^2}\right)_{z=0} z^2 + \text{----}}{\cancel{u} + \left(\frac{\partial u}{\partial z}\right)_{z=0} z + \left(\frac{\partial^2 u}{\partial z^2}\right)_{z=0} z^2 + \text{----}} \quad . \qquad (2.1a)$$

Retaining only the first nonvanishing terms gives

$$\frac{h_y\, dy}{h_x\, dx} = \left(\frac{\partial v/\partial z}{\partial u/\partial z}\right)_{z=0} = \frac{c_{fy}}{c_{fx}} \qquad (2.1b)$$

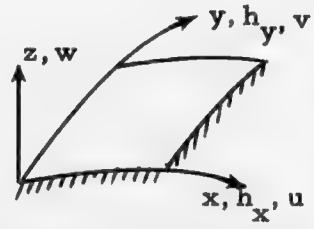

Fig. 2.1. Coordinate

which is just the skin friction lines (coordinates are indicated in Fig. 2.1). In the literature, both of the terms, limiting streamlines and skin friction lines, are used.

A point P(x, y) at which both c_{fx} and c_{fy} vanish is called a singular point of Eq(2.1b). Expansion of $c_{fx}(x, y)$ and $c_{fy}(x, y)$ around P yields, in general,

$$\frac{h_y\, dy}{h_x\, dx} = \frac{a_1 x + a_2 y + a_3 x^2 + \text{----}}{b_1 x + b_2 y + b_3 x^2 + \text{----}} \qquad (2.2)$$

Taking only the first-order terms, this equation exhibits a number of known singularity patterns (Fig. 2.2) that depend upon the relative

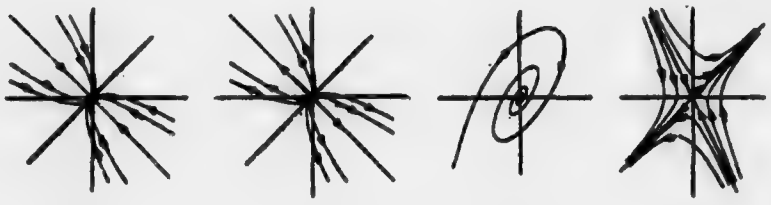

Fig. 2.2. Linear singularities

magnitudes among a_1, b_1, a_2, and b_2. Such linear (and also nonlinear) singularities are extensively studied in the fields of ordinary differential equations[9] and nonlinear vibration[10] in connection with phase-plane study. In any case, such singularities of the limiting streamlines have been frequently observed in surface-flow visualization experiments and, to a much lesser degree, some actually have been calculated. A nodal or saddle point (Figs. 2.2a, b, d) of attachment or separation is easier to comprehend intuitively; a spiral point of separation involves a more complex flow structure.

Recognition of the possible existence of such singular patterns is only a first step. The real question is which singularities occur in a given flow and where are they located; whether a saddle point, for example, is located on the windward or leeward symmetry-plane for an inclined body of revolution can significantly change the separation pattern. A further question is how the separation between singular points is connected. Indeed, for three dimensions, one asks whether the separation line must pass the singular points. These questions will be discussed later.

2.2 Three-Dimensional Separation Criteria

A number of researchers have attempted to advance a proper definition or criterion for flow separation in three dimensions. In this process, it was guickly agreed that three-dimensional separation is fundamentally different from two-dimensional separation; its resolution requires new ideas. It was also recognized that the vanishing of skin friction, either one of two components or both, can not be used to define a three-dimensional separation. Beyond these, different versions of separation criteria stress different aspects. The search still continues to this date. The following table represents only a partial listing.

Hayes (1951): Inaccessible, validity of b. l. assumptions.

Moore (1953): Bubble, inaccessible.

Eichelbrenner & Oudart (1954, 1973): Envelope, inaccessible.

Maskell (1955): Envelope; bubble (singular) and free vortex layer (regular).

Lighthill (1963): A skin friction line through singular points (inaccessible).

Stewartson (1963, 1969): Envelope, inaccessible.

Wang (1970): Envelope, closed (inaccessible) and open (accessible).

The essential features of each author's criterion are also indicated.

When a flow separates, the boundary layer assumptions are certainly no longer valid. This is true in two- as well as three-dimensional flows. However, such invalidity is not a precise criterion of separation and it is inconvenient to implement.

The concept of "bubble" and "inaccessibility" are carried over from the two-dimensional case. They are valid in certair circumstances, but do not hold in general as originally supposed. Also they provide only qualitative descriptions and these are inconvenient to implement.

The envelope idea has been specially developed for the three-dimensional case. It was first suggested by Eichelbrenner and Oudart[13] based on experimental surface-flow observations. Later numerious surface-flow results appear to support the concept. However, since the mathematical complexity prevents the determination of such an envelope exactly in any real flow problem, this envelope idea remains more a general statement than a precise criterion. This idea, by itself, does not enable one to determine separation uniquely. Additional descriptions of separation of a more specific nature are imperative.

Maskell[1] eluci dated considerably the envelope criterion and went further, classifying separation as a bubble type or a free vortex layer type. The former passes through the singular points, the latter contains only regular points. Here the terms "singular" or "regular" points refer to the limiting streamline equation (Eq. 2.1b) and should not be confused with the singularity of boundary layer equations. Maskell's work represents an outstanding contribution to the understanding of flow separation in three dimensions.

Lighthill[8] warned, however, that to "call the separation line an envelope of limiting streamlines is confusingly inaccurate." Instead, he defined a separation line as "a skin friction line which issues from both sides of a saddle point of separation and, after embracing the body, disappears into a nodal point of separation."

Following Lighthill's definition, the separation line, being itself a limiting streamline, is distinguished from other limiting streamlines in that it passes through the singular points. Other limiting streamlines do not meet the separation line except at the nodal point (Fig. 2.3a).

Since it is a closed curve around the body, the separated region would be inaccessible to flow from the upstream, unseparated region. In contrast, based on the envelope definition, limiting streamlines may meet the separation line anywhere along the line (Fig. 2.3b),

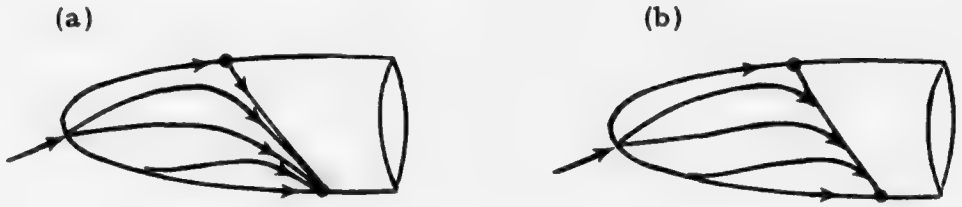

Fig. 2.3. Streamline (a) and envelope (b) as the separation line.

and the separation line *is not necessarily associated* with the inaccessibility idea.

Stewartson[15, 5] argued in support of the envelope concept. He cited the mass-flow relation derived by Lighthill himself,

$$\frac{1}{2}\,(c_{fx}^{2} + c_{fy}^{2})^{\frac{1}{2}}\, z^{2}\, h = \text{const.} \qquad (2.3)$$

where c_{fx} and c_{fy} are the components of skin friction, z is measured normal to the body, while h is the distance between two adjacent, limiting streamlines. For a streamtube of width h, and height z immediately above the body, the average velocity becomes $\frac{1}{2}(c_{fx}^{2} + c_{fy}^{2})^{\frac{1}{2}}z$ and Eq. (2.3) states simply that the volume flow along the streamtube is constant. Then there

are two mechanisms through which the streamlines may lift off the surface (i.e., as z increases). Namely: either both skin-friction components vanish or h becomes so small that the limiting streamlines approach each other. The latter leads to the envelope concept.

While Stewartson favored the envelope concept, he, like Hayes and others, stressed the notion of inaccessibility. He defined a separation line "as a curve on the body dividing those points that are accessible to the streamlines entering the zone at attachment from those points that are inaccessible from attachment." He further stated "this definition is appropriate whether the separation skin friction is singular or otherwise."

In contrast, the present author[16, 17] also favors the envelope idea, but has introduced an open-and-closed separation concept. A closed separation is consistent with the inaccessibility mentioned above, but an open separation can be just the opposite. Therefore accessibility is not a proper criterion of separation. We discuss next the open-and-closed separation concept in detail, and indicate how this idea evolved. In Section 3, support from recent calculations and surface-flow experiments will be discussed.

2.3 Open vs. Closed Separation

The essential idea can be best explained by considering a body of revolution (Fig. 2.4a, b) for which there is a plane of symmetry. Extension to general situations is straightforward. Fig. 2.4a illustrates

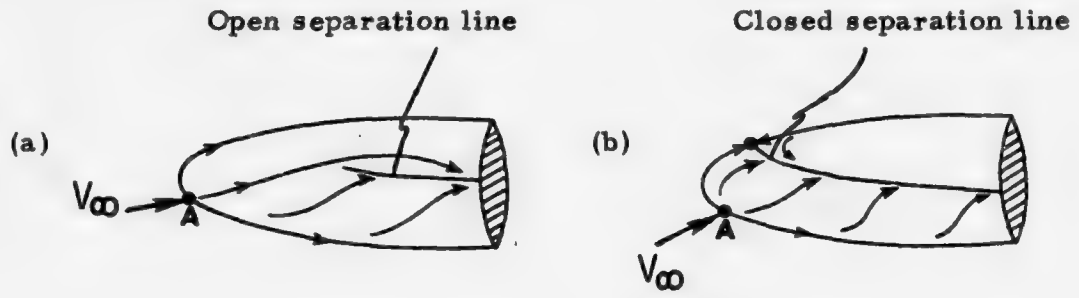

Fig. 2.4. Open vs. closed separation.

an open separation; Fig. 2.4b, a closed separation. Point A is the front attachment (or stagnation) point. By an open separation we mean that the separation line is not closed in the front leeside surface and does not originate or terminate at singular points in the sense that both skin friction components vanish. The limiting streamlines on both sides of the separation line originate from the same front attachment point; i.e., the separated region is accessible to upstream flow. In contrast, for a closed separation, the separation line is closed around the body, passing through the singular points of the limiting streamlines so that the limiting streamlines on two sides of the separation line originate from two different attachment points.

The concept of a closed separation is familiar, but that of an open separation is new. Separation of two-dimensional problems can all be interpreted in the present context as of a closed type simply by

visualizing a two-dimensional body as an infinite cylinder whose axis is perpendicular to the undisturbed flow direction. The idea of an open separation first evolved from a boundary layer study along the symmetry plane of an ellipsoid of revolution at incidence.[18,19] In that work, profiles

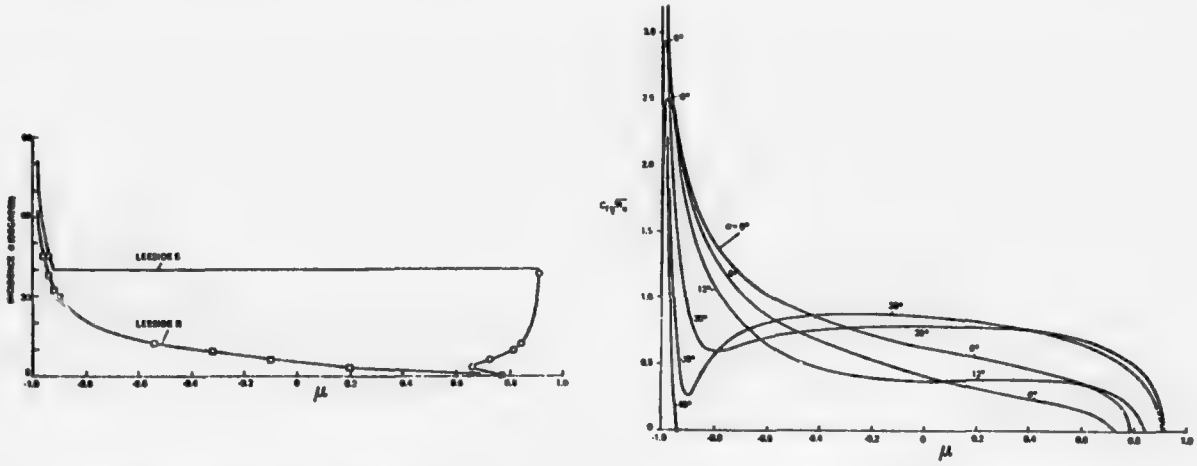

(a) Movement of R and S (b) Leeside c_f distribution

Fig. 2.5. Symmetry-plane boundary layer.

of the meridional velocity, u, and of the lateral derivative of v, $\partial v/\partial\theta$ were calculated (v is the circumferential velocity). The vanishing of $\partial u/\partial z$ and $\partial(\partial v/\partial\theta)/\partial z$ on the body surface determines the separation point, S, as usually defined and the starting point of circumferential flow reversal, R. The movement of points R and S on the leeside for an ellipsoid of $b/a = 1/4$ is shown in Fig. 2.5a where μ is the meridional coordinate. As the incidence increases, point R moves continuously forward, point S first moves forward and later rearward, and then, at still higher incidence, it jumps to the front end and moves slowly forward thereafter. This behavior follows from the leeside skin friction distribution shown in Fig. 2.5b[19].

The skin friction first exhibits a minimum at the forebody, and then this minimum grows deeper and finally reaches zero at ~40° incidence. Such rearward movement and the discontinuous jump of S suggest, among other things, a new feature of flow separation and presents a striking contrast to the two-dimensional case shown in Fig. 1.2.

At a fairly high incidence (say 30°), reversal of the circumferential flow becomes strong and moves forward toward the nose. Under such circumstance, it was thought that separation might be expected to have occurred away from the symmetry-plane region along the body. Near the symmetry plane, however, since the point S remains at the rear, there is no mechanism to provide a closed separation at the front. Based on this argument it was concluded that the separation must be open.

As just indicated, the open-vs-closed separation concept was originally conceived on the basis of a symmetry-plane boundary layer study. However since then, concrete examples of open separation have appeared in the literature, both from numerical solutions of complete three-dimensional boundary layers and from surface-flow visualization experiments. These will be presented in Section 3.

The question of the conditions under which open separation might occur is, of course, interesting, but difficult to answer in precise terms. What is known now is that open separation prevails over smooth elongated bodies of revolution at small (but not zero) to moderate incidence. The word "small" and "moderate" are only relative terms and vary with other parameters. The bodies referred to include, for example, ellipsoid of revolution, blunt cone, and hemisphere cylinder (Section 3). For such geometry, the velocity and the adverse pressure gradient of the lateral flow can be large or comparable to those of the longitudinal flow.

Corresponding to these features, the lateral body dimensions normal to the free stream, h and d, are smaller than the streamwise dimension, L. Remember that in the limit of zero incidence, separation, if it occurs, is known to be closed. Here the scales h, d, L are described in projected dimensions in order to account for the yaw or incidence effect (Fig. 2.6a).

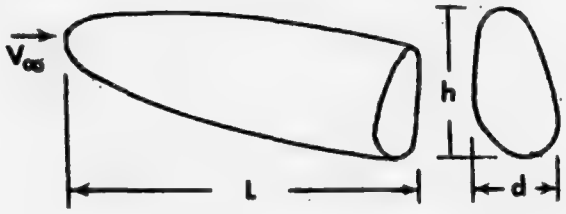

Fig. 2.6a. Geometry for possible open separation.

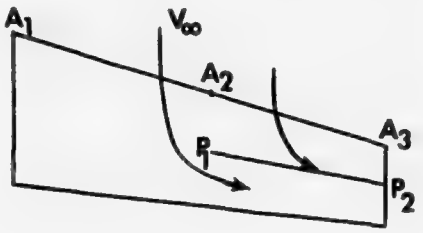

Fig. 2.6b. Part-span separation.

The front nose radius in our consideration is not necessarily a characteristic length. The hemisphere-cylinder serves as a good example. The nose bluntness may cause a short separation bubble, while the main separation, which occurs over the long afterbody is of open type, and is affected by the overall length.

When there is a front stagnation line rather than a stagnation point, the situation will be somewhat different. There, the meaning of "open" or "closed" becomes less precise and depends on which part of the limiting streamlines one may refer to. This happens in the case of a swept wing (Fig. 2.6b). The separation line P_1P_2 may extend only over part of the span (see Fig. 4 of Ref. 1). In our terminology of "open" vs "closed" separation, P_1P_2 is closed with respect to the limiting streamlines passing through the part of the leading edge A_2A_3, but it may be considered as "open" with respect to the

limiting streamlines through the part A_1A_2 because these limiting streamlines may reach the backside of P_1P_2.

In an open separation, the separation surfaces, one on each side of the leeside symmetry-plane of an inclined body of revolution, are not connected and form something like a channel on the leeside. In a closed separation, a single surface usually encloses the separation

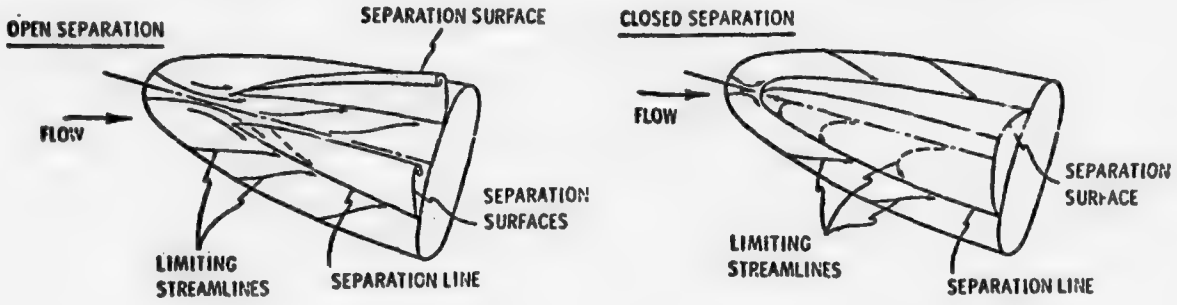

Fig. 2.7. Consequence of open vs closed separation

region, at least, for some axial distance from the front, and appears on the leeside as a "bubble," a term carried over from two-dimensional problems.

It seems reasonable to expect the following: An open separation readily leads to the shedding of vortices and the formation of a large wake. In contrast, associated with a closed separation, the vortices are embedded inside the bubble and are smaller in extent and weaker in strength. Furthermore, the bubble remains attached to the body, so that wake formation is delayed. Wake vortices can cause flow unsteadyness, asymmetry, and other complications. A closed separation is, therefore, preferred to an open separation from this viewpoint. This can be achieved by avoiding an intermediate range of incidence and/or increasing the body thickness.

2.4 Summary View of 3-D Separation

A number of alternative criteria which have been proposed were discussed in Section 2.2, followed by a discussion of the concept of open and closed separation (Section 2.3).

The definition of separation as an envelope of limiting streamlines appears most likely to be correct. Surface-flow experiments tend to support this definition and limited calculated results also suggest it. Rigorous mathematical proofs remain to be made.

Further classification of three-dimensional separation can be made from other viewpoints. For example, one may alternatively speak of "open" vs "closed", depending on whether the separation line (or surface) at the front is open or not; "singular" vs "regular," depending on whether the separation line contains the singular points or not; and "channel" vs "bubble" with emphasis on the shape of the separation surface; "free" vs "fixed" and so on.

Maskell classified the separation as "bubble" vs "free vortex layer." The same terms were used by this author[16] as well. Nevertheless it seems that "bubble" is a term descriptive of the shape, while "free vortex layer" stresses the structure of the separation surface. Actually all separation surfaces are a kind of vortex sheet in structure, although there is a difference in whether the sheet is free or fixed in some sense. We prefer to speak of "closed vs open" separation, which describes the main intuitive feature, and present an especially striking contrast to the "inaccessibility" notion usually associated with separation.

The idea of "open vs closed" separation is compatible with Maskell's concept of "bubble vs free vortex layer" separation. However

the specific idea of "openness" was not discussed by Maskell nor by other authors. For example, Stewartson[5, 15] has argued in support of Maskell's ideas, but he, in turn, stresses "inaccessibility" as the separation criterion in direct contrast to "openness." The terms "open" and "closed" were used by Maskell to describe the streamlines. These should not be confused with the "open" and "closed" separation lines referred to here. Whether a separation line is open or closed is a different matter as to whether a streamline is open or closed.

Reversal of one component flow (say, either longitudinal or lateral) of a three-dimensional boundary layer does not necessarily signify separation. So long as the rule of the zone of dependence[20, 21] is satisfied, calculation of such reversed flow does not contradict the basic idea of an initial-value problem. This is because reversal of one component of the flow is not the same as reversal of the resultant flow. Indeed, for a three-dimensional boundary layer, the flow direction (parallel to the body surface) varies across the layer at a given point on the body surface, hence sweeping out some solid angle. A distinctive flow direction does not exist. The dependence rule, which requires the computation mesh to enclose the solid angle, ensures precisely the satisfaction of the initial-value concept.

3. BODY-FLOW SEPARATION

In this section, separation patterns over inclined bodies are presented. Three-dimensional effects are most pronounced for this geometry. The open separation discussed in Section 2 is also most apparent here. The majority of this section is devoted to evidence supporting such open separation.

The case of a supersonic pointed cone will be dealt with first, but an ellipsoid of revolution is chosen to illustrate the general characteristics of body-flow separation. The blunt cone and hemisphere cylinder are two configurations common in aerospace application and their separation pattern can be inferred from that for an ellipsoid of revolution.

3.1 Supersonic Pointed Bodies

This problem of a supersonic sharp cone was first considered by Moore[12] and has since been investigated both numerically and experimentally by numerous investigators. Some variations of this problem include pointed ogives and cones of noncircular cross-section. Primary separation of a supersonic cone has been well established, with consistent and conclusive results from a variety of investigations. It occurs along a cone generator, entirely due to the reversal of the cross flow. The separation lines move away from the windward symmetry-plane with increasing incidence until the incidence reaches some limit. After that,

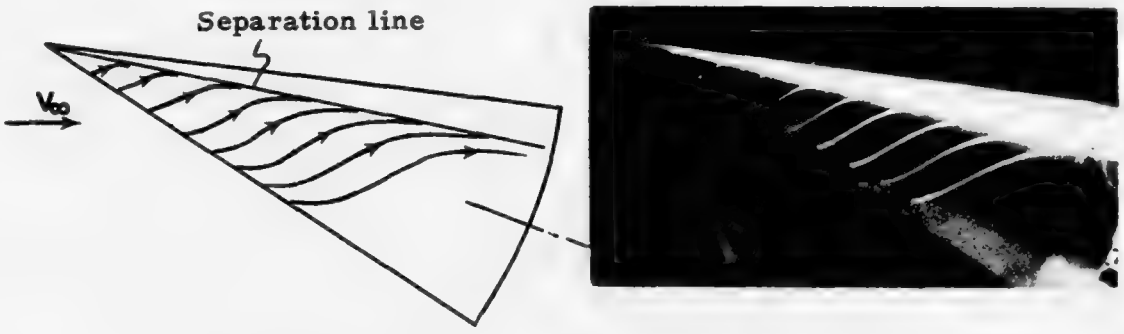

(a) Sketch of (b) (b) Surface flow (Werle[31])

Fig. 3.1. Separation over a sharp cone.

it moves no further. Recent full three-dimensional boundary layer calculations for this kind of problem have been reported, for example, in Refs. 22-25.

3.2 Ellipsoid of Revolution

The incompressible flow over an ellipsoid of revolution contains most of the essential elements of boundary-layer interest. It is a finite body smoothly closed at both ends, so that both favorable and adverse pressure gradients occur along both the longitudinal and lateral directions.

3.2a. Separation Sequence

Fig. 3.2 depicts a sequence of the side view of the separation pattern over an ellipsoid at increasing incidence. These sketches are for the case where the ratio of minor/major axes is $\frac{1}{4}$. The cases of $\alpha = 0^\circ$, 6°, 30°, and 45° are based on full three-dimensional calculations[17, 26, 27], while the intermediate cases of $\alpha = 3^\circ$, 15°, 40°

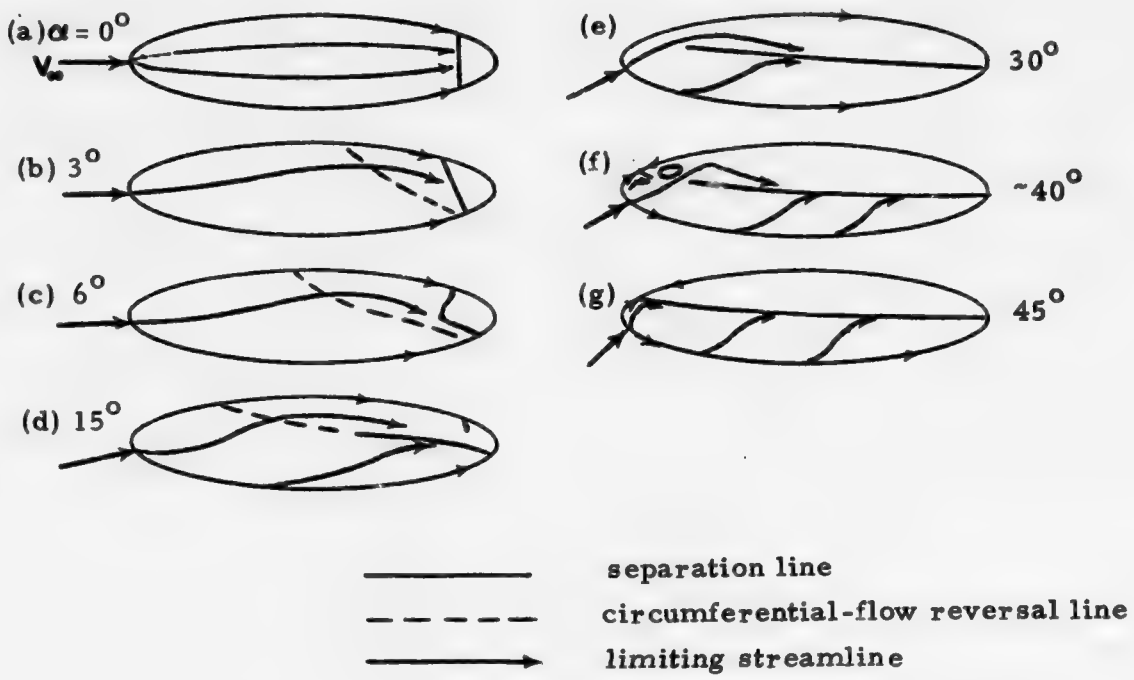

Fig. 3.2 Sequence of separation

are based partly on the general trends and partly on implications from Hsieh's experiment[28].

At zero incidence (Fig. 3.2a), an axisymmetrical flow separates at a fixed parallel. Small increase of incidence (3°) tilts the separation line slightly. It is preceded by a small region of weak reversal of the circumferential flow (Fig. 3.2b).

As the incidence further increases (say 6°, Fig. 3.2c), the leeside separation point moves rearward rather than forward so that the

separation line is bent as shown in an enlarged view (Fig. 3.3a). The

(a) Near breakup (b) After breakup

Fig. 3.3. Initiation of open separation.

upper branch AC inclines rearward, whereas the lower branch CD inclines forward. Meanwhile, the reversal of the circumferential flow starts ahead of the mid-body on the leeside (see Fig. 3.2c).

At higher incidence, the separation line breaks so that the lower branch CD extends forward to become what we call an open separation line as shown in Fig. 3.2d and enlarged in Fig. 3.3b. The change from a closed separation at low incidence to an open separation at higher incidence thus evolves gradually. It is difficult to pinpoint at what particular incidence this change takes place. Even for 6^{o} incidence (Fig. 3.2c and Fig. 3.3a), it is difficult to say whether the separation line is closed in the section BC.

After an open separation occurs, what happens to the flow immediately behind the broken separation lines AB and CD, and for

that matter, the separated flow over the afterbody, is not understood. It is conjectured, however, that there may exist tail vortices (Fig. 3.3b) analogous to the nose vortices to be discussed later (Section 3.6).

Meanwhile, the reversal of circumferential flow becomes more strong, and its starting point, R, on the leeside continues to move forward (Fig. 2.5a). The separation line can be approximately identified with the circumferential-flow reversal line although it is located slightly aft.

The open type of separation persists as the incidence continues to increase (say 30°, Fig. 3.2e). The separation line continues to stretch forward, but otherwise the basic pattern remains the same.

Following the stage at which the singular separation points, S, on the leeside symmetry-plane jumps to the front nose (as discussed in Section 2.3), new features start to appear (Fig. 3.2e). Near the point, S, a local saddle-point flow pattern develops; meanwhile, the open separation line moves close to the symmetry plane. At this juncture, there is a possibility that a concentrated vortex may appear at the nose (see Section 3.6).

Finally, as the incidence continues to increase (about 45° in this case), the separation becomes completely closed. Increase of incidence thereafter does not greatly change the pattern.

Thus, we have arrived at a systematic sequence of development of separation for an inclined body. As the incidence increases, the separation changes through a cycle: from closed to open and back to closed. For the example shown here (ellipsoid of $b/a = \frac{1}{4}$) the range of incidence for the cycle runs from 0° to 45°. A more slender

ellipsoid of revolution is more sensitive to the incidence variation so that the corresponding cycle may take place at considerably lower incidence. On the other hand, for a sufficiently fat ellipsoid of revolution, the separation will be always a closed type.

The foregoing discussion can be carried over to shapes differing from the ellipsoid. In the case of a blunt cone or a hemispherical cylinder, for example, the fore-body flow develops the same way and differences arise only over the afterbody. When the afterbody is of conical or cylindrical shape, the separation occurs roughly along a generator and hence becomes less complicated.

3.2b Calculated Results

Wang's calculations [17, 26, 27]. The laminar boundary layer over an ellipsoid of revolution was calculated for the axis ratio of $\frac{1}{4}$ at 6°, 30°, and 45° incidences. Results are shown in Figs. 3.4a-e. where the body surface is represented in a plane rectangular coordinate system consisting of meridional distance, μ, and circumferential angle θ. In Figs. 3.4a, b, c, the separation lines are shown along with the limiting streamlines, inviscid surface streamlines, minimum pressure line, and the zero-$c_{f\theta}$ line which marks the beginning of the circumferential-flow reversal.

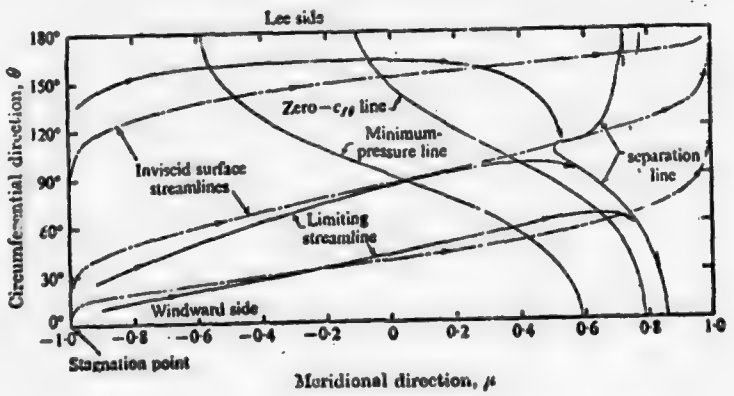

Fig. 3.4(a), $\alpha = 6^{\circ}$

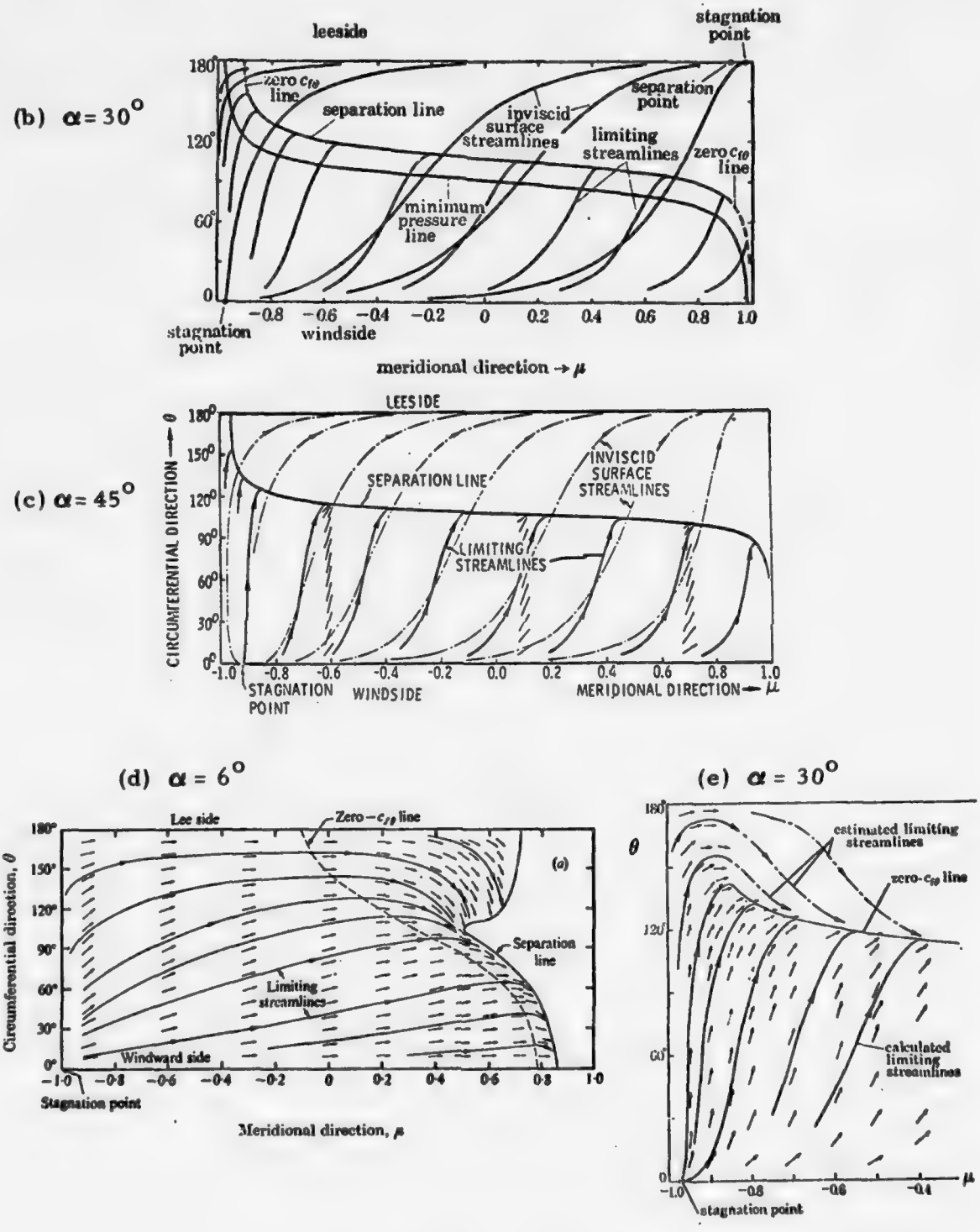

Fig. 3.4. Calculated separated lines.

The separation lines determined here agree well with envelope concept. At higher incidences (30°, 45°), they are close to the zero-$c_{f\theta}$ lines; at lower incidence (6°), the separation line is far from the zero-$c_{f\theta}$ line.

Fig. 3.4b further shows that the zero-$c_{f\theta}$ line does not signify separation near the ends of the body. Near the rear end, however, the separation point in the windside symmetry plane is so close to the zero-$c_{f\theta}$ line that there is not much value in making the distinction. Near the front end, the separation line is not closed, and hence an open separation prevails. Fig. 3.4e is an enlarged view of the fore body in Fig. 3.4b and is shown to display the open separation idea. The arrows indicate the calculated surface flow directions, and the limiting streamlines are drawn therefrom. Fig. 3.4d gives detailed surface flow conditions for Fig. 3.4a, especially in the reversed circumferential-flow region between the zero-$c_{f\theta}$ line and the separation line.

As the calculated limiting streamlines approach the separation line, they make a sharp turn and merge into the latter. This lends support to the concept that the separation line is the envelope of limiting streamlines rather than a limiting streamline itself.

The minimum pressure lines are also superimposed in Figs. 3.4a, b. Along this minimum pressure line both meridional and circumferential pressure gradients vanish. The minimum pressure line was once suggested as an approximation to the separation line. At lower incidence, this approximation fails badly; at higher incidence, the minimum pressure line is closer to the calculated separation line. However, such a crude approximation can not cope with the open separation flow structure.

Geissler's calculation [29]. Three-dimensional incompressible laminar boundary layers over ellipsoids of revolution and over a half-ellipsoid with cylindrical afterbody were calculated. Sample results of the calculated separation lines are shown in Fig. 3.5. All are of the

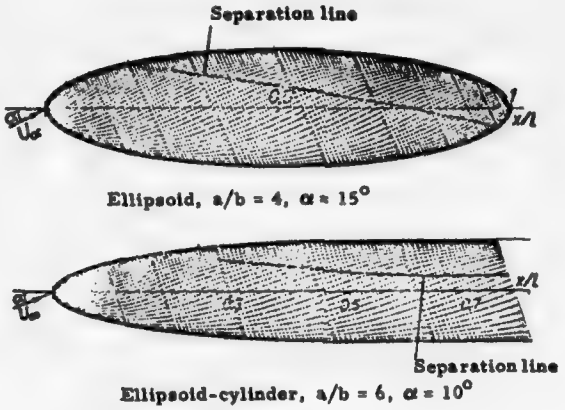

Fig. 3.5. Geissler's calculated separation lines.

open type and hence are in qualitative agreement with our preceding discussion of the open separation.

3.2c. Experimental Results

Peake, Rainbird and Atraghji [2] presented an oil dot surface-flow picture (Fig. 3.6a) for an ellipsoid of b/a = 1/6. The test was conducted at 25° incidence. The Mach number is 0.74 and the Reynold number is 44×10^6 based on the body length. The boundary layer is turbulent. Although the oil-flow picture is rather indistinct, the separation lines

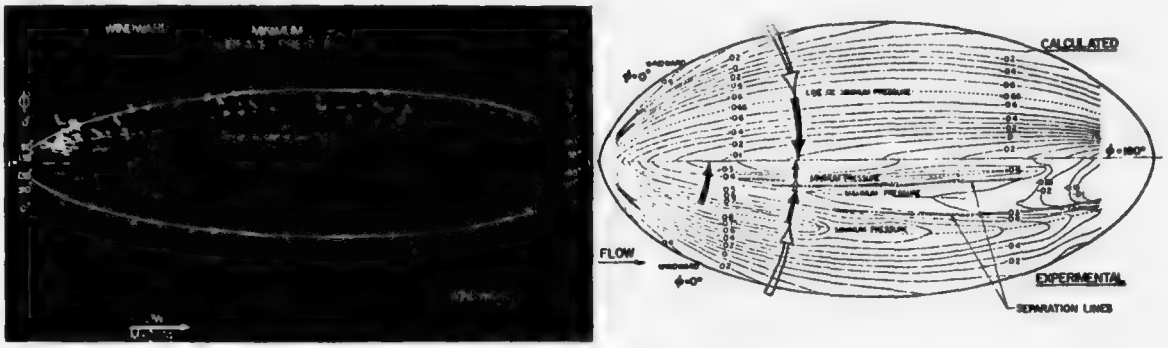

(a) Oil dot surface flow (b) Isobars and separation lines

Fig. 3.6. Ellipsoid separation (Peake, Rainbird and Atraghji).

and attachment line can be identified. Over the front nose, it is difficult to visualize whether the separation line is closed or open. The accompanying drawing by these authors (Fig. 3.6b), however, suggests that the separation is open.

Earlier, Eichelbrenner[13,30] reported a number of surface-flow visualizations for various ellipsoids, but the photographs are not clear enough to indicate a well-defined separation line. This led to certain incorrect description of separation as later pointed out by this author[16]. During the Viscous Flow Symposium at Lockheed-Georgia, 1976, Dr. V. C. Patel from the University of Iowa showed a color surface-flow slide for an ellipsoid of revolution with $b/a = \frac{1}{4}$ at 20° incidence and an open separation was clearly indicated.

3.3 Blunt Cone

3.3a. Separation Sequence

The separation pattern over blunt cones follows closely that for an ellipsoid of revolution, excluding the complications due to a contracting afterbody. At low incidence (typically say less than 4°), no separation occurs (Fig. 3.7a). At moderate incidence (6°~ 7°), an open separation starts to form over the rear portion (Fig. 3.7b). This pattern extends

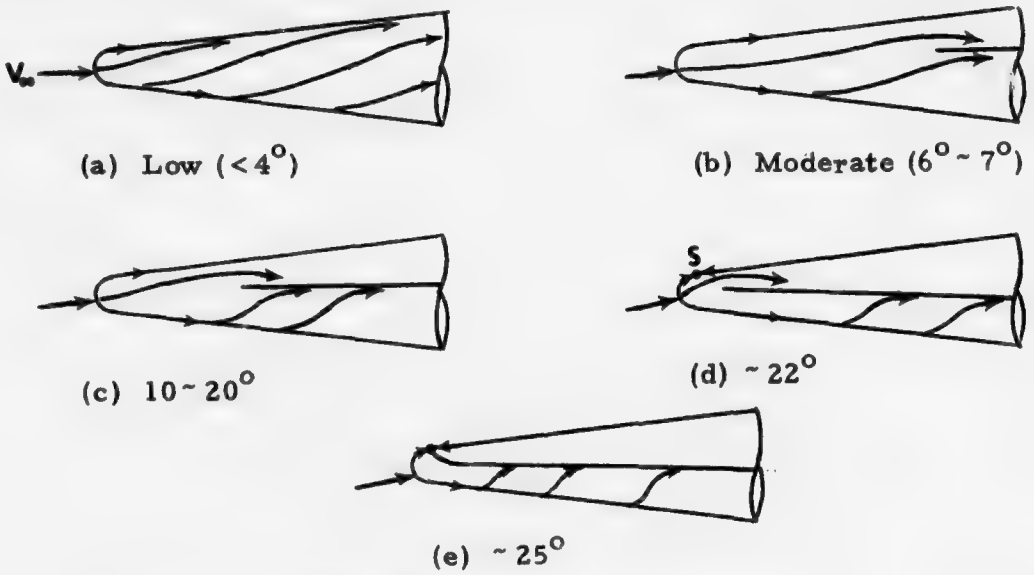

(a) Low ($<4^{\circ}$)

(b) Moderate (6°~ 7°)

(c) 10°~ 20°

(d) ~ 22°

(e) ~ 25°

Fig. 3.7. Separation sequence for blunt cone.

forward (Fig. 3.7c) as the incidence increases. At some point (say about 22°), a saddle-point may emerge near the front nose (Fig. 3.7d), resulting in the formation of a concentrated vortex to be discussed later. At still higher incidence, the separation quickly becomes closed (Fig. 3.7e). This sequence of development should hold for reasonably slender blunt cones. The specific range of incidence up to 18° is based on Stetson's[32,33]

experiment for the case of 30% bluntness (ratio of the nose-to-base radius). Above 18°, it is estimated by the author. The incidence range for the sequence will decrease as the blunt cone becomes more slender. Blunter nose shapes are discussed in Section 3.5.

3.3b. Experiment Results

Surface-flow separation experiments have been made by many investigators, including Werle[31], Stetson[32, 33], Zakkay[34] and others. Stetson's experiments provided the first convincing evidence compatible with our idea of an open separation.

Figs. 3.8a, b show oil-flow photographs at incidences of 10° and 18°. The model was a 5.6° half-angle cone with 30% nose bluntness at a Mach number of 14.2 and a free-stream Reynolds number per foot of 0.62×10^{6}. These pictures clearly demonstrate the open type of

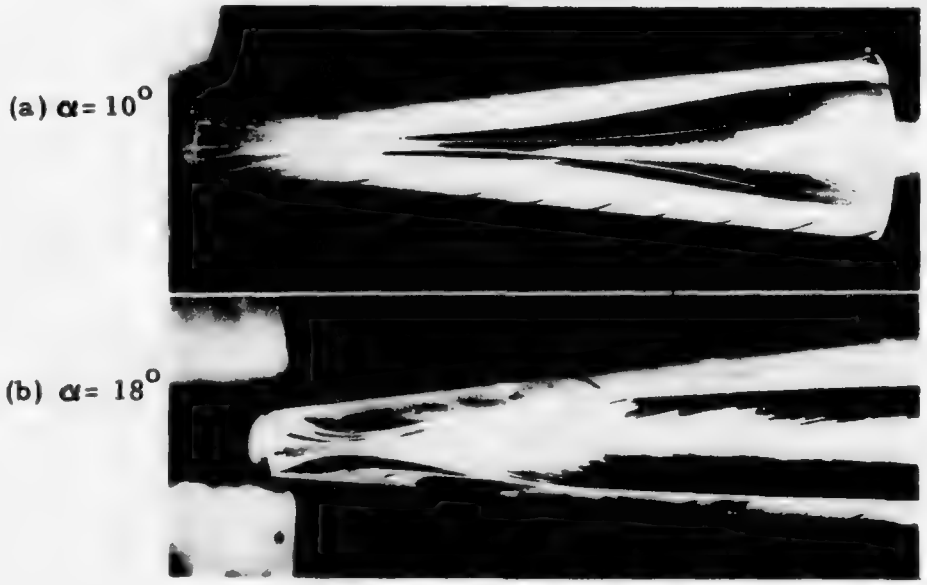

Fig. 3.8. Open separation on blunt cone, top view (Stetson).

separation. In Fig. 3.8a, two oil streaks proceed from the nose region directly into the separation region. A model of 10% bluntness was also tested by Stetson and yielded similar results.

Similar surface-flow experiments on blunt cones were reported by Zakkay et al.[34] and his general conclusions are much the same. Calculation of three-dimensional viscous flow over a 15^{o} half-angle blunt-cone at 15^{o} incidence has been reported by Lubard [35]. The separation line is not shown, but an open separation is indicated.

3.4. Space Shuttle

Flow separation patterns on the leeside of a space shuttle orbiter model were investigated by Zakkay, etc.[34] at a free-stream Mach number of 6. The free-stream Reynolds number ranges from 1.64×10^{7} to 1.31×10^{8} per meter, and the incidence angle varies from 0^{o} to 40^{o}. The cross section of the main body (exlcuding the wing) is nearly circular in the nose region, but gradually flattens on the sides and the bottom as one moves aft.

At 10^{o} and 20^{o} incidences, the separation was found to be an open-type. At 30^{o} and 40^{o}, it was of the closed type. Figs. 3.9a, b show the leeside surface-flows for incidences of 20^{o} and 30^{o}, where both the primary and secondary separation lines can be clearly identified. Over the rear portion of the model, the primary separation line remains straight and resembles that of a cone despite the presence of the wing.

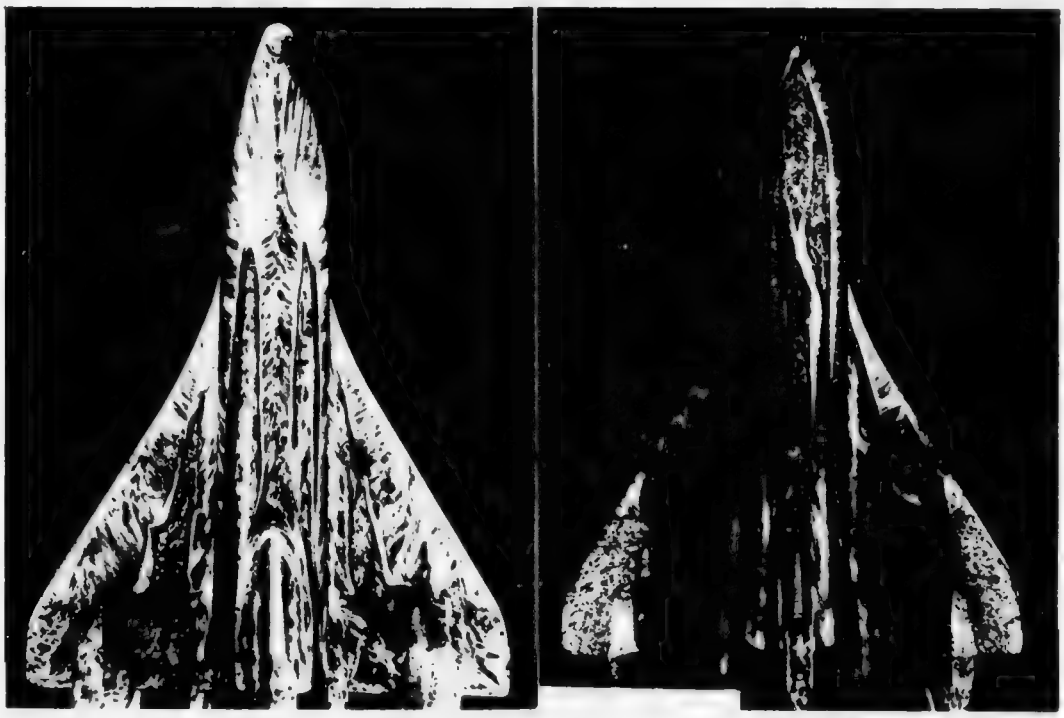

(a) Open separation, $\alpha = 20^{\circ}$

(b) Closed separation, $\alpha = 30^{\circ}$

Fig. 3.9. Separation on space shuttle (Zakkay, Migazawa and Wang).

This investigation provides further confirmation of the idea of an open separation under more general conditions; the body is not simply a body of revolution and the boundary layer involves laminar, transitional and turbulent flow. The conclusion on the general trend of the separation pattern, however, agrees well with our description based on the incompressible laminar solution for an ellipsoid of revolution.

3.5 Hemisphere Cylinder

The hemisphere cylinder represents a slight variation in geometry from the blunt cone discussed before, and finds wide application in missile design. Surface-flow experiments for a hemisphere cylinder were undertaken by Hsieh[36] at Mach number 0.6 to 1.4 and at incidence angles of 0° - 19°. The resulting separation patterns follow closely those described herein for an ellipsoid of revolution, and a blunt cone.

The sequential change is illustrated in Figs. 3.10a-d. The same sequence was found to hold for all Mach numbers tested. At zero

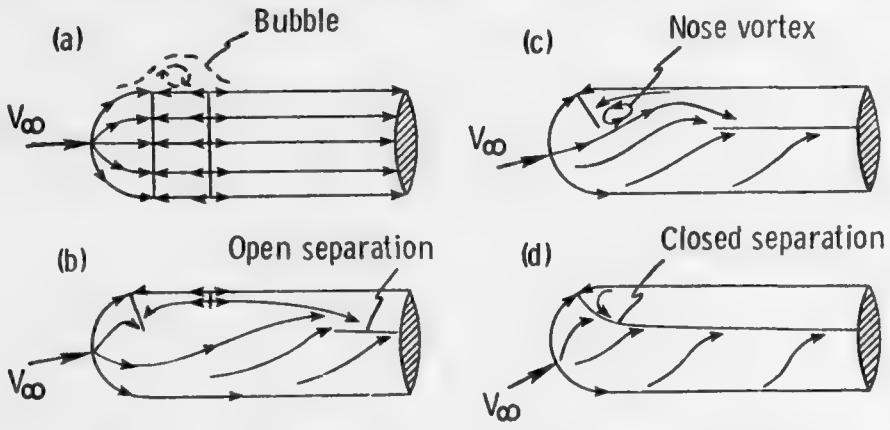

Fig. 3.10. Separation over a hemisphere cylinder.

incidence, a short separation bubble appears at the junction of the hemisphere and the cylinder (Fig. 3.10a) and represents the only departure from the previous cases. At lower incidence (say 4° ~ 5°), the separation bubble on the windward surface gradually disappears, whereas that on the leeward surface moves slightly forward. Meanwhile, an open separation line starts to emerge over the aft-body (Fig. 3.10b). As the incidence further increases, (say 10°), the open separation line extends farther forward. At 15° - 19°, a concentrated vortex may appear on the nose, as discussed later. It is expected, but not yet tested experimentally, that

continuing increase of incidence would lead finally to a completely closed separation (Fig. 3.10d, estimated to be around 25° for this case). Figs. 3.11a-c show surface-flow photographs for M = 1.2. An open separation line over the rear body is barely visible in Fig. 3.11a, and extends forward and can be clearly identified in Figs. 3.11b, c.

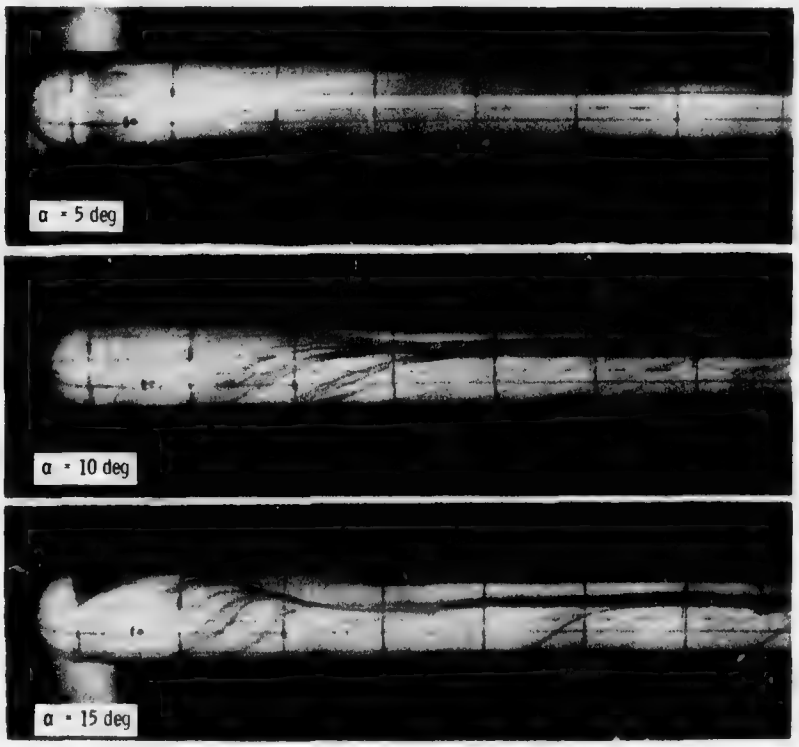

Fig. 3.11. Open separation over hemisphere-cylinder (Hsieh).

3.6 Nose Vortices

A vortex pattern on the leeside front nose of an inclined body of revolution (Fig. 3.12a) was first revealed in Werle's surface-flow experiments in 1962[31]. During the following years, no similar vortex

(a) Werle, M = 0, $\alpha = 20^{\circ}$ (b) Hsieh, M = 1.0, $\alpha = 15^{\circ}$

Fig. 3.12. Nose vortices.

was reported, and little additional understanding of this problem developed. Recently, however, a similar pattern was observed by Hsieh[36], as mentioned in the preceding section. The latter led to the suggestion by Hsieh and Wang[28] of a possible mechanism to explain the formation of such a nose vortex within the context of the open-and-closed separation idea. As illustrated in Figs. 3.2 and 3.10, and further enlarged in Fig. 3.12c, with the progressive increase of incidence to a

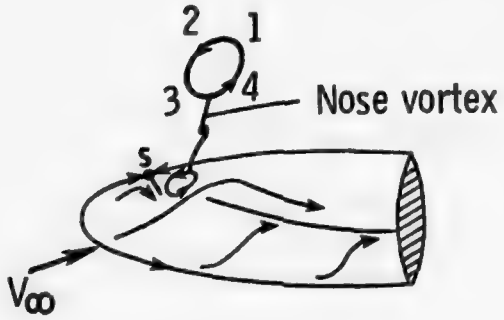

Fig. 3.12c. Enlarged sketch of nose vortex.

certain stage, the open separation line extends forward, coming very close to the leeside symmetry-plane. A local separation starts at the saddle separation point, S, if there is no short bubble separation as in the hemisphere cylinder case. At this point, a counter clockwise circulating vortex path can be formed; the reversed flow caused by the short bubble or the local separation near point S follows the upper path ($1 \rightarrow 2 \rightarrow 3$, Fig. 3.12c), while the open separation permits the flow to enter the leeside region along the lower path ($3 \rightarrow 4 \rightarrow 1$). If the incidence is increased further, the separation would become completely closed, and the vortex would disappear. Based on this reasoning, the vortex can be expected only during the transition from an open separation to a completely closed separation. It is, of course, understood that there is actually a pair of such nose vortices, symmetrically situated on two sides of the plane of symmetry.

4. WING-FLOW SEPARATION

Analytical study of three-dimensional boundary layers was first started for the case of an infinite yawed cylinder.[6, 7] Being independent of the spanwise coordinate, the chordwise flow can be determined exactly as for a two-dimensional airfoil, while the spanwise flow can be determined separately afterward by a linear equation. This simplified model provides important insight to three-dimensional character and has since been widely used. However, rigorous solution of the genuine three-dimensional boundary layer for a finite wing is still lacking.

Our discussion on separation here relies on surface-flow experiments and on intuition. A great variety of wing-flow separations have been reported. Particularly interesting is the predominant spiral-vortex pattern over a finite swept wing at high incidence. Unfortunately, such patterns cannot be determined by boundary layer solutions; instead they require solution of the Navier-Stokes equations. The transonic swept wing is distinguished by shock-boundary layer interactions. The delta wing is usually known for its characteristic leading-edge separation, but the surface-flow pattern for the case without leading-edge separation is equally interesting. These cases will be discussed in the order mentioned.

4.1 Infinite Yawed Wing

Wild's work[37] represents a classical one of the infinite yawed wing problem. He calculated an elliptic cylinder at 7° incidence; the ratio of the major to minor axes is 6:1, and the yawed angle is 45°.

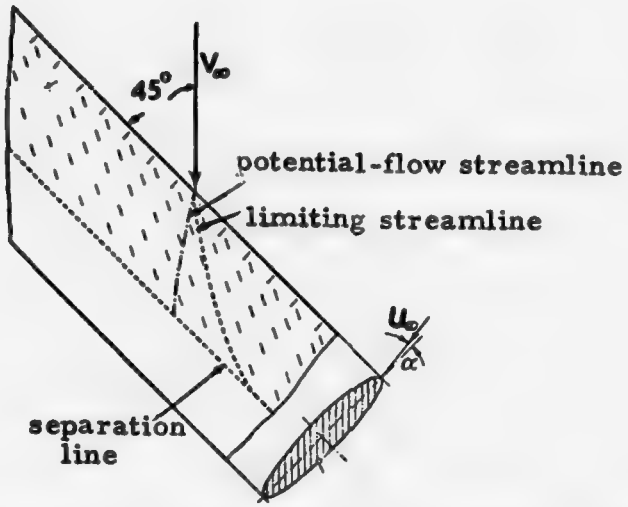

Fig. 4.1. Separation over an infinite yawed wing (Wild)

Results are shown by the short-line segments in Fig. 4.1 which indicate the calculated local limiting flow directions. These results agree well with tuft observations. The limiting streamlines show a strong outward departure from the inviscid surface streamlines, a unique characteristic of three-dimensional boundary layer effects. The separation line is determined by the vanishing of the chordwise skin friction.

4.2 Subsonic Swept Wing

4.2.a Low Incidence Case

Separation over a typical finite swept wing of moderate to large aspect-ratio at low incidence follows closely that of an infinite yawed wing, except near the tip and root. Separation occurs nearly parallel to the trailing edge (Figs. 4.2a, b). Fig. 4.2a is intended to be a simplified sketch of Fig. 4.2b which was reported by Vanino and Wedemeyer[38, 39]. The wing has an aspect-ratio of 4.8, and was tested at M=0.7 and $\alpha = 6^\circ$. A typical tip vortex pattern can be seen near the tip.

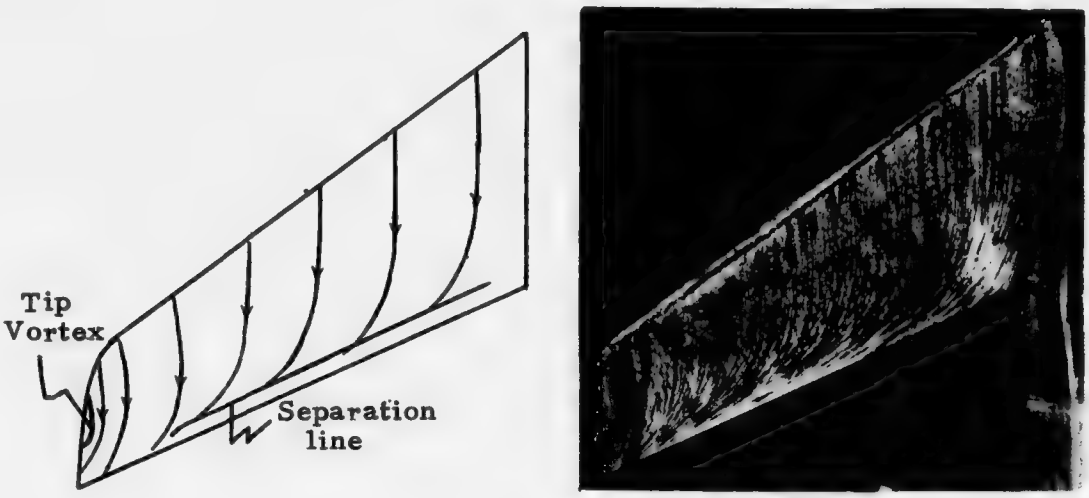

(a) Sketch of (b)

(b) Surface-flow (Vanino and Wedemeyer)

Fig. 4.2. Separation over swept wing at low incidence.

A sharp leading edge always causes separation along the leading edge. Leading-edge bubble separation also may occur. Very often, it extends along the span somewhere behind the leading edge. The boundary layer then becomes turbulent and reattaches. Leading edge bubbles may also break into segments along the span[40].

4.2.b. High Incidence Case

Wing flow is especially sensitive to change of incidence. As the incidence increases over a few degrees, the separation can become entirely altered. Fig. 4.3a sketches a spiral surface-flow pattern which has been

consistently observed and represents a typical wing separation pattern at higher incidence. It consists of an inboard spiral vortex pattern and an outboard saddle-point pattern. Above the surface, a part-span vortex spirals downstream. Fig. 4.3.b portrays a different part-span separation sketched by Lighthill[8].

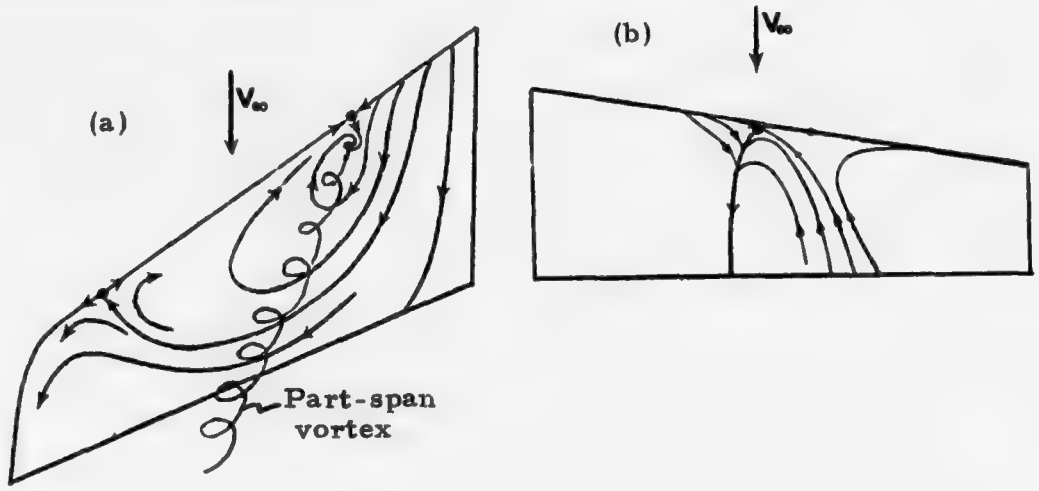

Fig. 4.3. Separation over swept wing at high incidence.

The oil-flow picture[41] in Fig. 4.4 displays a clear spiral pattern, and represents an early experimental observation of this type of wing-flow separation. A vortex arising at a part-span station and trailing downstream is visible. At the present time, little is known about the mechanism for the occurrence of such spiral flow.

Fig. 4.4 Spiral surface-flow separation (Cooke and Brebner).

Figs. 4.5a-c[38, 39] are top views of a more systematic development of the spiral surface-flow pattern at a Mach number of 0.7. The planform has an aspect ratio of 3, and a sweep angle of 25°. At 8° incidence (Fig. 4.5a), there appears to be a leading-edge short-bubble separation; otherwise a nearly two-dimensional chordwise flow pattern prevails, except at the tip region which will be discussed later.

At 10° incidence, an increase of 2°, the surface flow pattern becomes entirely different (Fig. 4.5b). A spiral pattern similar to that in Figs. 4.3a and 4.4 can be clearly visualized. The center of such a spiral vortex can also be discerned at a part-span station near the leading edge. The short-bubble separation appears to extend only inboard of the vortex center parallel to the leading edge. Upon further increase of incidence to 14° (Fig. 4.5c), the spiral vortex appears to

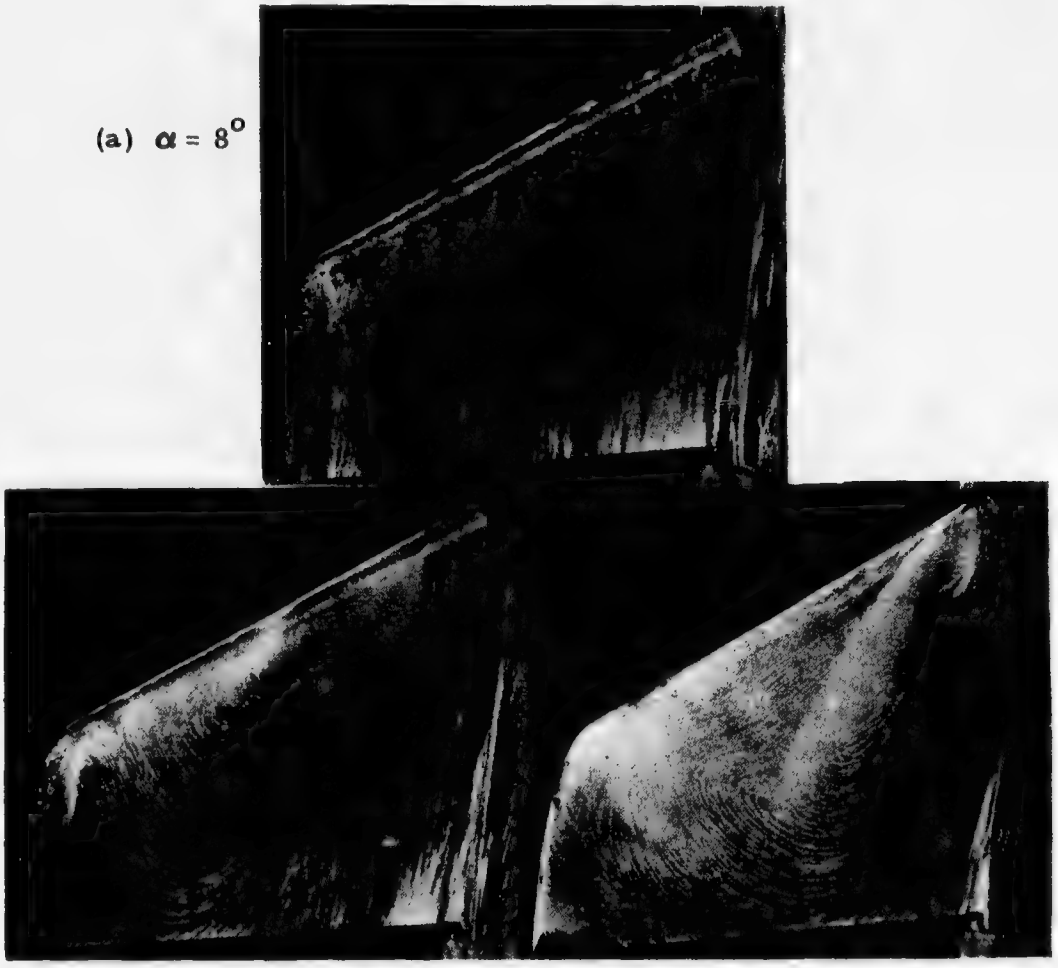

(a) $\alpha = 8^{\circ}$

(b) $\alpha = 10^{\circ}$

(c) $\alpha = 14^{\circ}$

Fig. 4.5. Surface-flow patterns over swept wing (Vanino and Wedemeyer).

become much stronger, and its center shifts toward the root of the wing. The vortex trailing backward above the wing' s surface is especially clear in this picture, and the leading-edge bubble separation disappears completely.

The surface-flow pattern near the tip is dominated by the tip vortex. Figs. 4.6a, b, c are sketched corresponding to Figs. 4.5a, b, c. In Fig. 4.6a, a large vortex pattern covers the tip region. In addition, there appears a short chordwise separation line (i.e., a

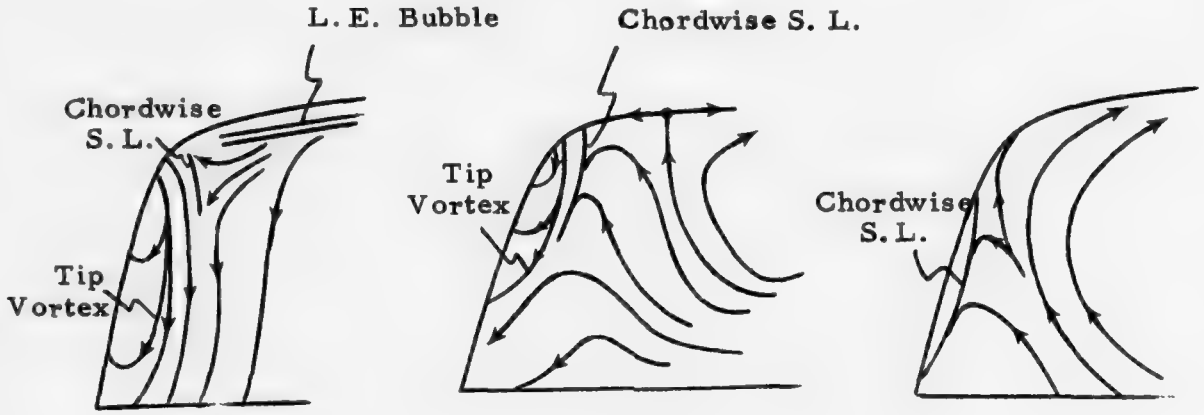

(a) $\alpha = 8^{\circ}$ (b) $\alpha = 10^{\circ}$ (c) $\alpha = 14^{\circ}$

Fig. 4.6. Tip-flow pattern.

separation line runs along chordwise), and a leading-edge separation bubble. As the incidence increases to 10° (Fig. 4.6b), the tip vortex moves forward and shrinks in size, whereas the chordwise separation line becomes longer. At 14° incidence (Fig. 4.6c), the tip vortex disappears altogether, and the chordwise separation line runs almost along the edge of the wingtip. The spiral vortex pattern becomes strong enough to dominate the whole upper surface of the wing.

It has been observed[43] that the part-span vortex shifts inboard (see Fig. 4.7a) with increasing angle of incidence, decreasing Reynolds

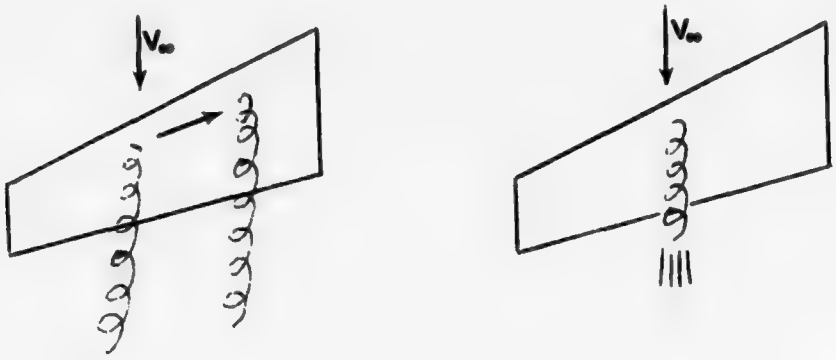

(a) Inboard shift (b) Breakdown

Fig. 4.7. Factors after part-span vortex.

number, decreasing leading-edge radius, and increasing leading-edge sweep angle. The part-span vortex may break down early or trail behind the wing for some distance. Experiments indicate that the vortex breaks down earlier with decreasing sweep and increasing incidence.

4.3 Transonic Swept Wing

The transonic wing flow[42, 43] is characterized by the presence of a mixed subsonic-supersonic flow, shock waves, shock-boundary layer interaction, and the resulting extended separated region.

There are basically three shocks (Fig. 4.8a): forward, rear, and outboard. The forward shock originates near the leading edge of the wing root and runs downstream toward the tip. The rear shock originates near the trailing edge of the wing root and runs upstream toward the tip. The outboard results from the merging of the first two,

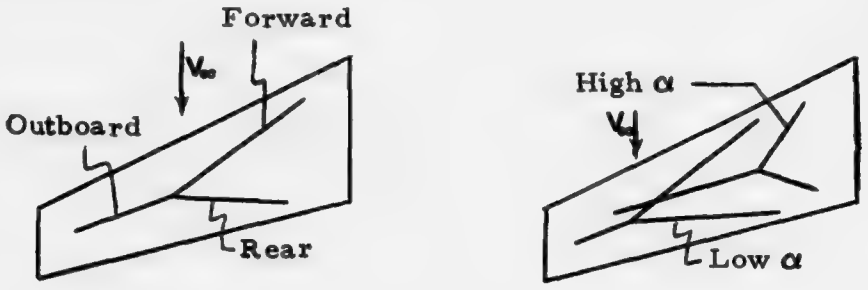

(a) Basic three shocks (b) Effect of incidence

Fig. 4.8. Shock system on a transonic wing.

and hence, is stronger. As the incidence increases, the forward shock shifts downstream (Fig. 4.8b) and the rear shock shifts upstream, so that the outboard shock extends farther toward the wing root.

A weak outboard shock may cause a bubble separation and/or a kink deflection on the limiting streamlines (Fig. 4.9a), but a strong

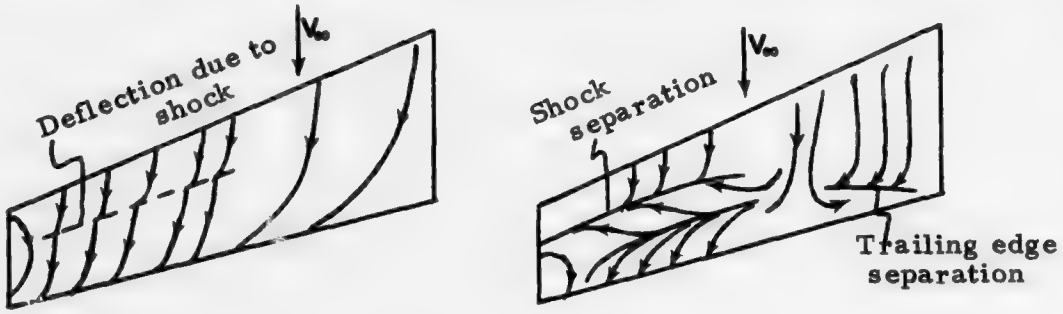

(a) Flow deflection due to shock (b) Shock and T. E. separations

Fig. 4.9. Surface flow over a transonic wing.

outboard shock leads to flow separation. Hence over a transonic wing, the outboard separation is due to shock, whereas if inboard separation occurs, it is an ordinary trailing-edge separation. As these two separation lines do not necessarily join together, a strong spanwise flow may enter into the separated region. As the incidence increases, the shock separation line moves closer to the leading edge.

Figs. 4.10a-d[38, 39] show a series of shock separation patterns.

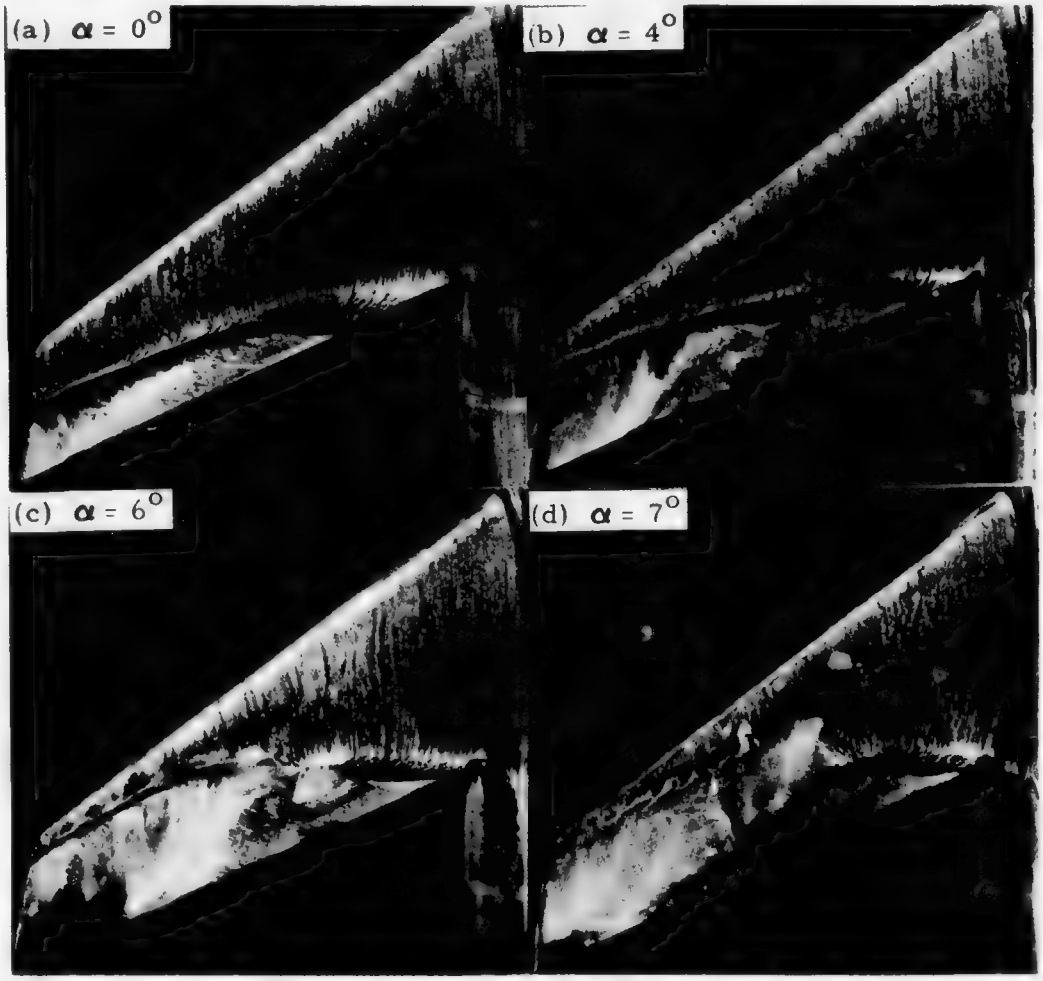

Fig. 4.10. Separation over a transonic wing (Vanino and Wedemeyer).

The wing aspect-ratio is 4.8, the sweep angle is 35° and the Mach number is 0.95. At zero incidence (Fig. 4.10a), the shock separation takes place outboard in the trailing edge area. As the incidence increases (Fig. 4.10b), the shock moves toward the leading edge while the separated region spreads. In Figs. 4.10c, d, an inboard trailing-edge type of separation can be seen in clear distinction to the outboard shock separation, and the two do not join together. These pictures are not clear enough to indicate a definite flow pattern inside the separated region. Further increase of incidence would move the shock ahead of the wing, and it is expected then that the surface-flow pattern would resemble those shown in Figs. 4.3a and 4.5c -- i.e., a predominant spiral-vortex pattern.

4.4 Delta Wing

4.4a With Leading-Edge Separation

A delta wing with a sharp leading edge is characterized by a leading edge separation regardless of the speed range. Leading-edge separation occurs also on highly-swept delta wings with round leading-edges. A typical situation is illustrated in Fig. 4.11. The primary separation occurs at the leading edge as a pair of vortices symmetrically set on the leeside. The flow spirals around these two vortices and reattaches along the line A . In the middle, the surface flow is conical. Secondary separation occurs along the line S_1 and reattachment along A_1. Although such a flow has not been calculated, and details of the structure remain to be studied, a qualitative picture of Fig. 4.11 has been well established through many experiments (for example, Refs. 44, 45).

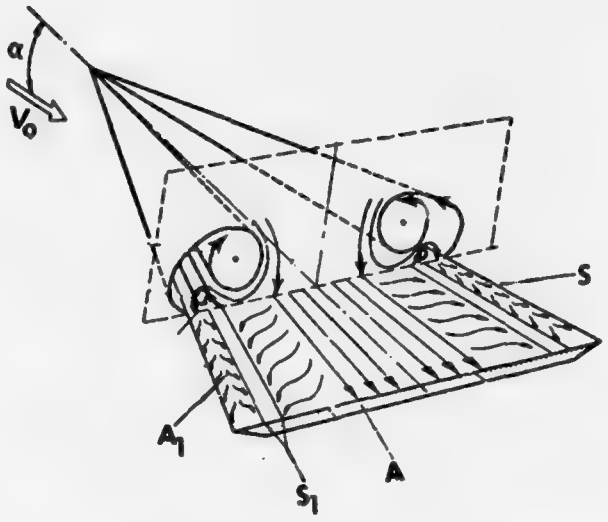

Fig. 4.11. Delta wing separation (Werle[45]).

Leading-edge separation and the associated loss of lift and increase of drag should generally be avoided. However, for a slender delta wing configuration, such a penalty may be offset by a different consideration. Since the primary separation is permanently fixed to occur at the leading edge, this eliminates the uncertainty in separation prediction, avoids more complex separation which might otherwise occur, and simplifies control of a vehicle.

4.4.b Without Leading-Edge Separation

The surface-flow pattern over a delta wing without a leading-edge separation has not been well studied. Werle's work[45] is the only one of this kind known to this author. A sequence of development for this problem is illustrated in Figs. 4.11a-d sketched on the basis of Werle's

experimental pictures shown in Figs. 4.13a-d. Only the right half is shown. The top portion is much simpler in structure and is not illustrated

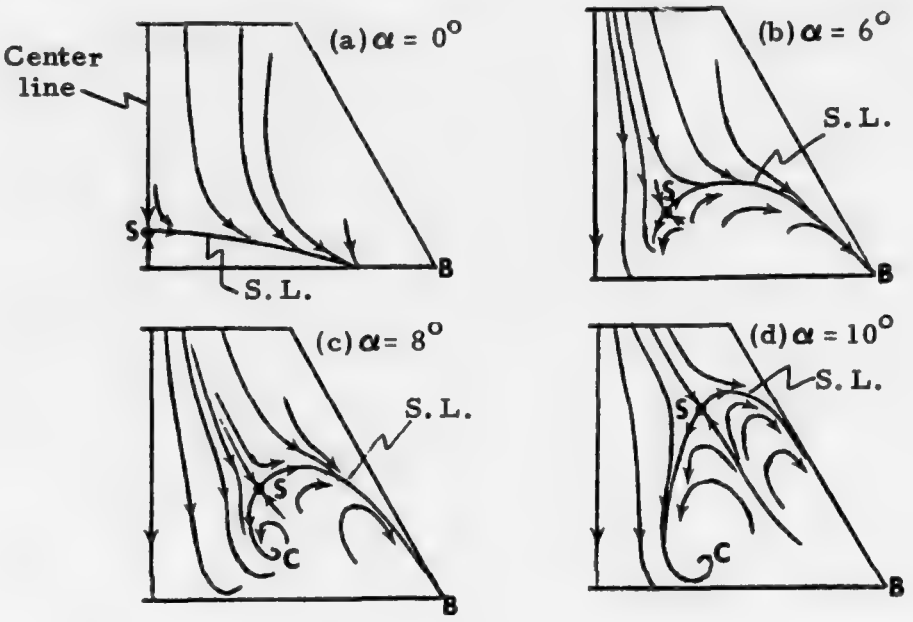

Fig. 4.12. Surface-flow pattern over a delta wing without leading edge separation. S.L. -separation line, C - spiral core, S - Saddle point.

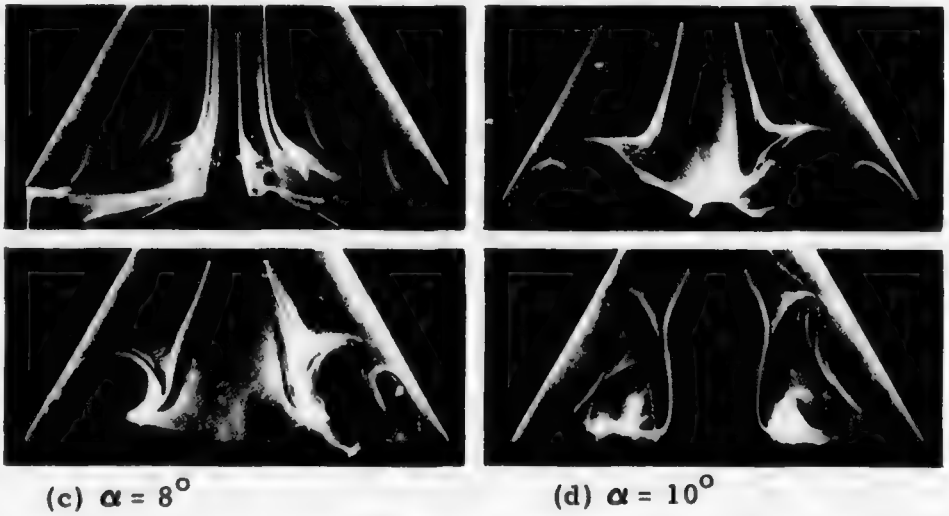

Fig. 4.13. Werle's experiment.

here. The wing has an elliptic spanwise cross-section, and a symmetric airfoil with a sharp trailing edge. The test conditions are M = 0 and $R_e \sim 10^4$.

At zero incidence (Fig. 4.12a), a saddle point S is located at the center line and a closed separation line is formed near the trailing edge. At 6^o incidence (Fig. 4.12b), the saddle point S has moved forward and away from the center line, and the separation line passing through S appears to terminate at one end at the wing tip B and at the other end at a spiral singularity C, although a spiral pattern is scarecely visible at this stage. The flow in the central position proceeds from the leading edge right through to the trailing edge, and goes outboard near the trailing edge to arrive at the backside of the separation line CSB. As the incidence further increases to 8^o and 10^o (Figs. 4.12c, d), the trend continues: the saddle point S continues to move up and away from the center line, the spiral pattern and its center C become more easily discernible.

5. CORNER-FLOW SEPARATION

The term "corner flow" problem[46, 47] originally referred to the more restricted case of a flow along the corner of two perpendicular

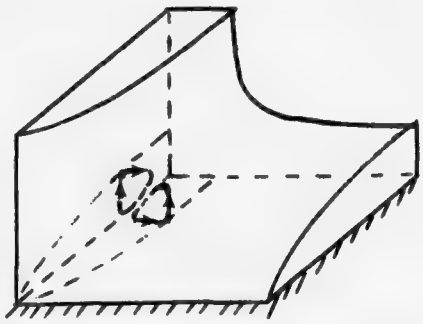

Fig. 5.1. Corner between two flat plates

plates (Fig. 5.1). It was treated by a modified boundary-layer approach. Away from the corner, a two-dimensional flat-plate boundary layer prevails. In the corner region, the two boundary layers interact to give rise to a pair of vortices. However, this problem has not been completely settled yet.

In the more general case, the corner is neither straight nor aligned with the oncoming flow direction. It occurs at junctions of any two connected bodies or from a protuberance on another body. Typical in aerospace applications is the junction of wing and fuselage or any control surfaces such as flaps, tails, etc. Other examples of corner junctions are the conning tower of a submarine and fins or flare on a projectile or missile. In these applications, the projecting body is long in comparison with the boundary-layer thickness. The corner problem for short protuberences (of the order of or less than the boundary layer thickness) is of interest in the transition study of roughness.

General corner flow is highly vortical in the sense that there are multiple vortices resulting from multiple separations and reattachments. Rigorous calculation of three-dimensional corner flow has required a complete Navier-Stoke approach and has not been practical to date. However, there have been numerous experimental investigations for protuberances normal to a base plate and under different flow conditions. Extensive bibliographs for this type of problem may be found in the survey articles by Korkegi[3], Sedney[48] and Ryan[49]. Most studies so far have been concerned with surface-flow visualizations, and with surface pressure and temperature distributions; very little has been done with respect to the flow structure.

Our present interest is limited to the separation patterns. We shall attempt to illustrate general features through a few typical examples. In the preceding two sections on bodies and wings, the separation pattern has been shown to vary widely with the change of the planform and incidence. On the other hand, corner-flow separation remains basically the same whether the perturberance is a cylinder, fin or flap. For all the cases considered, the separation is exclusively of the closed type.

5.1 Cylinder-Plate Corner

The flow over a circular cylinder normal to a flat plate has long been used as a model for viscous flow studies. It was first used to study three-dimensional boundary layers prior to separation, and later for the corner flow problem behind separation. In this author's opinion, this problem does contain the main features of general corner flow, and hence is a good

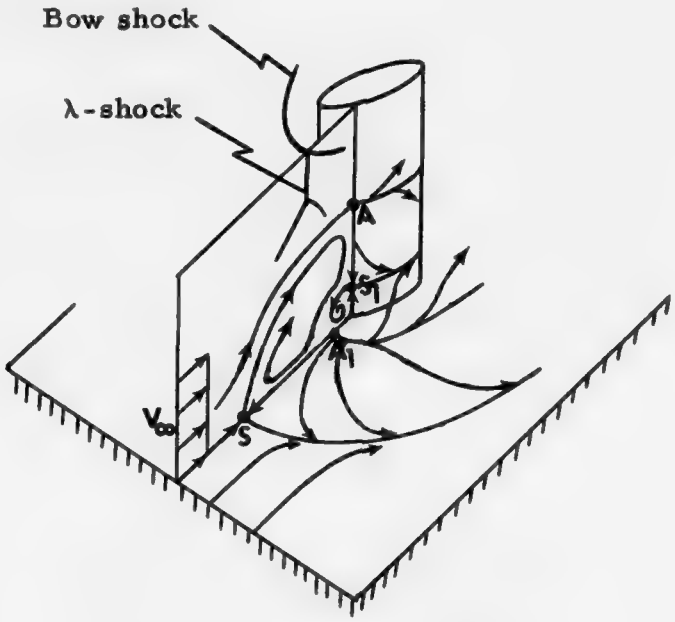

Fig. 5.2. Cylinder-plate separation

model for that problem. However, one cannot say as much for this problem as for a model for three-dimensional boundary layer study.

The cylinder-plate corner problem has been extensively investigated by experiments from incompressible to hypersonic flow under both laminar and turbulent boundary-layer conditions (for examples, Refs. 50-54). The separation patterns have been consistent in spite of the presence of the λ-shock in the supersonic to hypersonic speeds. Typically for a long protuberance (Fig. 5.2), the flow separates ahead of the cylinder and a reversed flow region immediately follows the separation. Above the plate, such reversed flow appears as a vortex which spirals away from the symmetry-plane downstream in the typical horsehoe form. The separated flow reattaches to the plate immediately ahead of the cylinder;

at the root corner, there appears a smaller counter-rotating vortex which also extends downstream as a horseshoe vortex. The attachment line has been described in the literature as a "herringbone" or "feather-like" pattern. Behind the cylinder there is a dead-water region with two counter-rotating vortices[54].

The flow pattern just described occurs most often. However, it has been known for some years that the number of vortices may be more than two when the length of the cylinder is shortened to be about the boundary layer thickness. This has been demonstrated most convincingly in

Fig. 5.3. Vortices in the symmetry-plane (Thwaites)*

the symmetry-plane flow[52] shown in Fig. 5.3. The smoke filaments in an incompressible flow show two large clockwise-rotating vortices. Each of these induces, in turn, a smaller counter-rotating vortex. As these vortices pass around the cylinder, they form horseshoe vortices. Thus there are two separation lines and two reattachment lines on the base plate.

---

*The author is indebted to Dr. L. C. Squire for the demonstration of this experiment during a recent visit to Cambridge.

In a series of tests for cylinders of different height and diameter, Sedney and Kitchens[54] found as many as six vortices. The cylinder they studied was 2.03 cm high and 7.62 cm in diameter, the Mach number was 2.50 and the unit Reynolds number was 3.0×10^6/m. The turbulent boundary layer on the wind tunnel wall was about 2.5 cm thick. Fig. 5.4

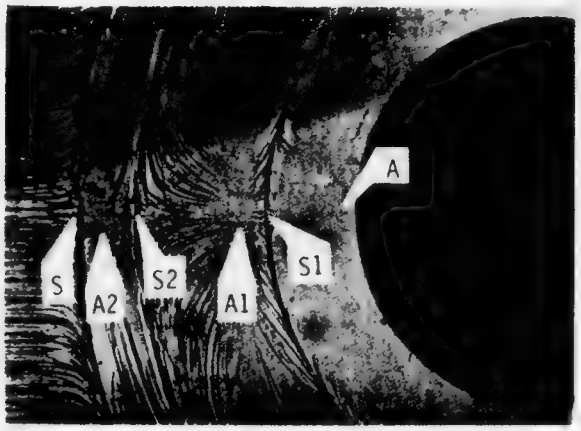

Fig. 5.4. Cylinder-plate
(Sedney and Kitchens)

shows a plan-view shadowgraph for the surface-flow pattern ahead of the cylinder. Three separation lines, marked as S, S_1, S_2, can be clearly seen. Three attachment lines, marked as A, A_1, A_2 are also discernible. A total of six vortices, three large and three small, is implied.

5.2. Fin-Plate Corner

The fin-plate corner problem also has received extensive experimental attention. A typical sketch for a blunt fin (based on Refs. 55-56) is shown in Fig. 5.5. The general pattern at the front portion is nearly

identical to that for the cylinder-plate corner in Fig. 5.2. The only noticeable difference is that, because the fin is a straight plate, it prevents the flow from closing behind it. In other words, the difference is mainly in the wake structure. Shown in Fig. 5.5 are two separation lines

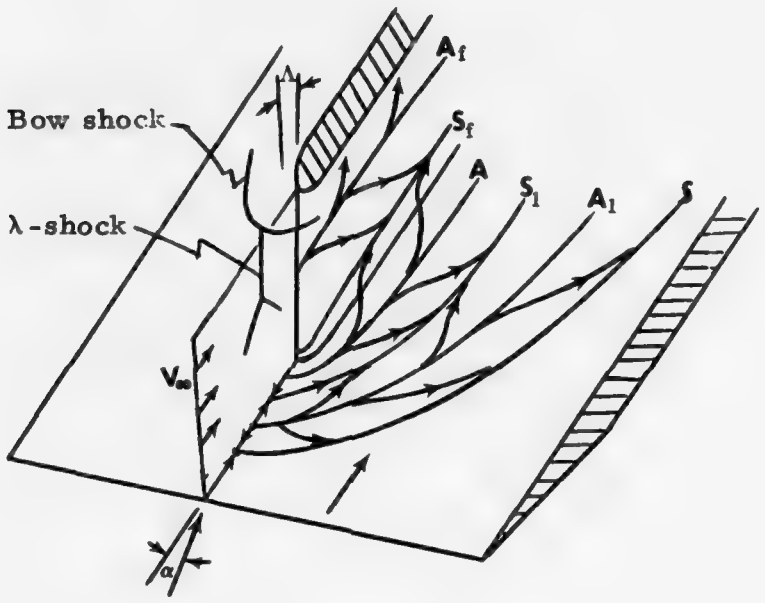

Fig. 5.5. Fin-plate corner separation
(Based on Refs. 55-56)

and two reattachment lines on the plate, as well as one separation line and one reattachment line on the side of the fin. Again the number of separation and reattachment lines on the base plate may vary just as in the cylinder-plate case before. Thomas[56] reported both single-and-two-stage separations on the plate. He also indicated that the fin surface flow suggests more vortices than just those based on the plate surface flow.

The fin-plate experiments include parameters such as the sharpness of the leading edges, sweep angles (Λ), and incidence angles (α). As Λ increases, separation may disappear altogether. As α increases, the plate leading-edge shock, which is stronger than the boundary-layer induced shock, interacts with the fin bow-shock. This mainly leads to higher heating on the fin but has less effect on the separation pattern with which we are concerned here.

A variation of this kind of corner problem is the case of two intersecting wedges in a supersonic flow considered in, among others, Refs. 57-59. This particular problem has received considerable attention.

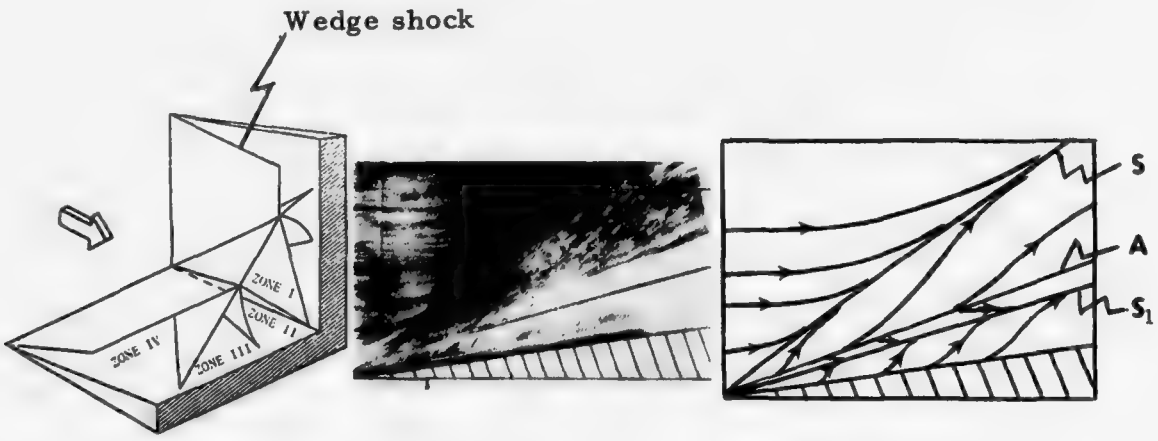

(a) Corner flow (Refs. 57, 58)

(b) Oil flow (Refs. 59, 3)

(c) Sketch of (b)

Fig. 5.6. Intersecting wedges

This configuration resembles somewhat the configuration shown in Fig. 5.1. However, the corner is not exactly aligned with the free stream. In addition the flow is supersonic. Particular interest in this problem centers around the complex shock system involving two wedge shocks, corner shock and inner shock. These shocks divide the corner flow into several distinct regions marked as I, II, III, in Fig. 5.6a. The flow in Region I is conical. The flow structure of Fig. 5.6a, first given by Charwat and Redekopp[58], has been confirmed by later experiments, although some minor modifications have been suggested.

The oil-flow[59] on the wedge surface when both half-wedge angles are 10° at $M_{\infty} = 20$ is shown in Fig. 5.6b. The Reynolds number is 3.35×10^{6}. The inner S-shaped line reflects a vortex, while the outer oil-accumulation line clearly indicates separation. In the middle, there is a feather-like pattern. Ahead of the separation is the usual two-dimensional wedge flow. Fig. 5.6c gives our sketch of Fig. 5.6b. There are indicated two separation lines, marked S and S_1, and one reattachment line, implying two larger vortices with a smaller one between. Korkegi[3] mentioned also a possible system of three vortices, presumably meaning that indicated in Fig. 5.6c. Watson and Weinstein[59] noticed earlier that such a feather-like pattern could be produced by counter-rotating vortices, although their interpretation differed from the present one. In Fig. 5.6c, due to the sharp edge, there is no separated region in front of the wedge.

5.3 Flap-Plate Corner

Flow separation due to a deflected control surface such as a flap has been extensively investigated throughout the Mach number range, especially for two-dimensional models. At a fixed Mach number, increase of unit Reynolds number decreases the separation length ahead of the flap. Increasing the Mach number while maintaining flap angle and unit Reynolds number tends to decrease the separation length.

A typical three-dimensional flap separation in front of a flap is illustrated in Fig. 5.7b, sketched on the basis of the accompanying oil-

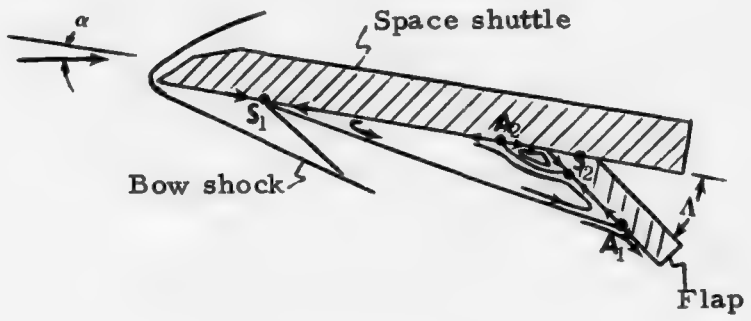

Fig. 5.7a. Shuttle at incidence (Cut-out view along the center line, from Goldman and Obremski)

flow picture, Fig. 5.7c. This experiment was reported by Goldman and Obremski[60] in a series of tests for studying the hypersonic buzz of a space-shuttle configuration (Fig. 5.7a). This particular geometry is included here because of the clear separation picture shown in Fig. 5.7c

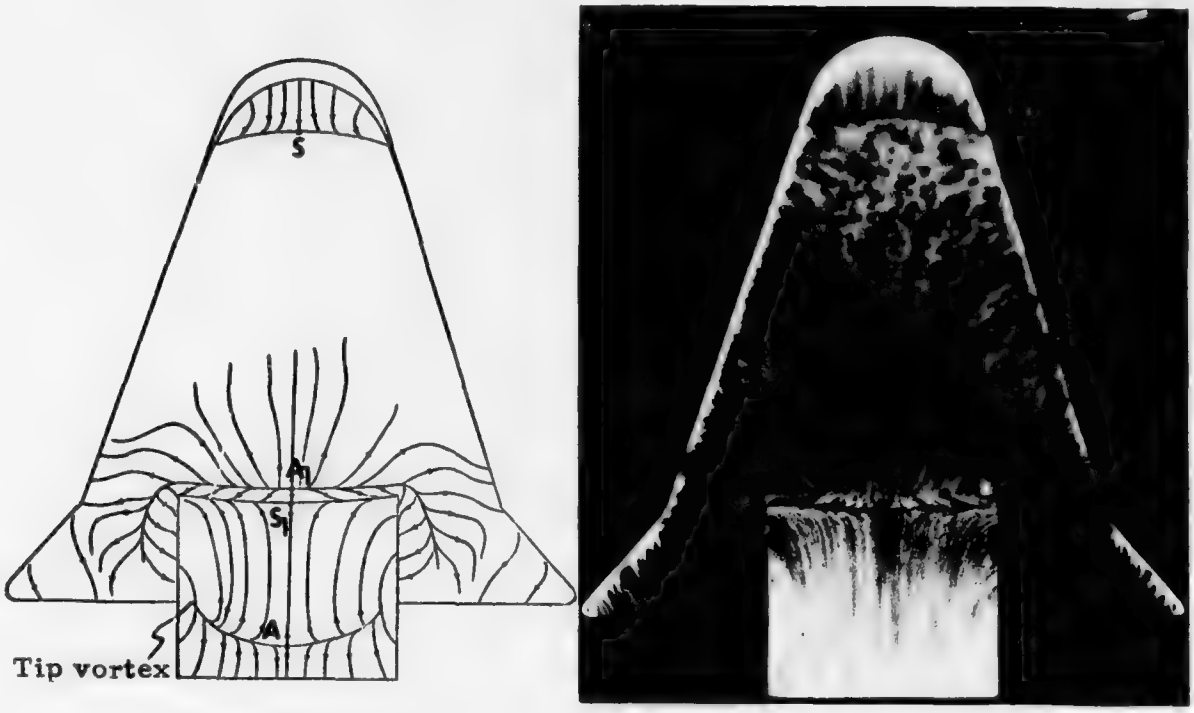

(b) Sketch of (c)

(c) Oil flow pattern, $\alpha = 10^{\circ}$, $\Lambda = 40^{\circ}$, $M = 17.5$

Fig. 5.7. Flap-Shuttle Separation (Goldman and Obremski)

which is believed to be fairly representative for general flap separation. For our purpose, we may merely consider the bottom side of the shuttle model as a flat plate with the flap inclined at an angle Λ.

Fig. 5.7c corresponds to conditions at M=17.5, $\alpha = 10^{\circ}$, $\Lambda = 40^{\circ}$, $Re = 15 \times 10^{6}$, and a laminar boundary layer ahead of separation. Separation occurs first at the forebody marked by S, and reattaches on the flap marked A. Near the flap root, a secondary separation and reattachment occur, marked S_1 and A_1. Along the center line, there appear to be two counter-circulating flows. They turn downstream along the reattachment line A_1 and form two horseshoe vortices. A feature unique to the present flap case, and in contrast to the preceding cylinder

and fin cases, is the flap' s tip vortices (Figs. 5.7b, c), resembling those for a finite wing.

Increase of incidence in the present model reduces the effective angle between the free-stream flow and the flap if Λ is kept constant. Then the separation line S, generally moves rearward, the reattachment line A, on the flap moves downward, and the secondary separation and reattachment, S_1 and A_1 may disappear altogether.

If the flap angle is large (say $\Lambda = 90^\circ$, $\alpha = 0$) and the height of the flap is short (comparable to the boundary layer thickness), then multiple stages of separation and reattachment may be expected to occur on the body (not the flap), similar to what were discussed in the cylinder-plate corner case.

5.4. Cone-Flare Corner

In the open literature, there appears to have been very little reported about the separation of the cone (or cylinder) -flare corner flow at incidence. This flow was not, for example, covered in the survey articles by Korkegi[3] and Sedney[48]. In general, change of incidence affects the flow over cylindrical bodies considerably and the same is expected to be true for the related corner flow.

Our discussion here follows the work of Harris[61] who investigated a series of spherically blunted 10° cones with 30° and 60° flares. Figs. 5.8a, b are oil-flow photographs showing the side view at $\alpha = 40^\circ$, $M_\infty = 9.75$ and $Re = 1.56 \times 10^5$. Figs. 5.8c, d are our sketches of Figs. 5.8 a, b. For $\Lambda = 30^\circ$, Fig. 5.8c indicates that the corner flow separated along line S_1 on the cone and reattached along line A_1 on the flare.

$\Lambda = 30^{\circ}$ $\Lambda = 60^{\circ}$

(a) (b)

(c)

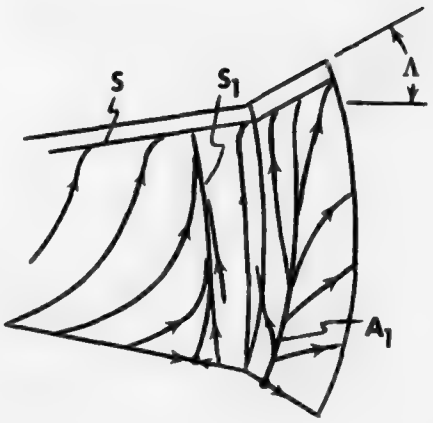

(d)

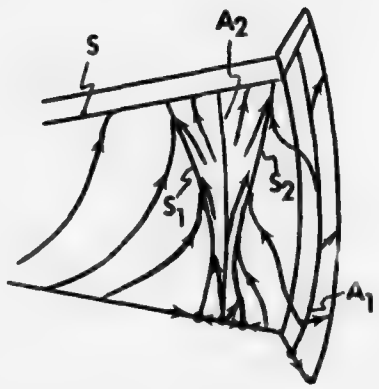

Fig. 5.8. Cone-flare separation, side view. S-body separation; S_1, S_2 - corner separation (Figs. 5.8a, b from Harris).

The separation line marked S on the leeside of an inclined cone was discussed in Section 3. For $\Lambda = 60^{\circ}$, Fig. 5.8d indicates that S_1 moves forward and that there is an additional stage of separation and reattachment on the cone marked S_2 and A_2. It is interesting to note that on the leeward surface, the line S_1 bends forward, whereas S_2 bends rearward. This latter behavior could hardly have been predicted. Thus there is one corner vortex for $\Lambda = 30^{\circ}$, but three for $\Lambda = 60^{\circ}$.

Harris further shows that for a fixed Λ at $\alpha = 0$, the separation line S_1 on the cone moves forward to some maximum as the bluntness ratio increase from zero, and then moves rearward with further increases in bluntness ratio. The latter is defined as the ratio of the nose to base radius at the cone-flare juncture. The same trend is believed to hold for α greater than zero.

6. CONCLUDING REMARKS

Separation patterns in three-dimensional flow are discussed here. Apart from our previous boundary-layer calculation results, most of the discussion relies on experimental observations and on intuition. For most of the cases examined, the separation patterns appear to be rather independent of whether the boundary layer is laminar or turbulent. Except for the transonic wing problem, the separation also does not depend on whether the flow is incompressible or hypersonic. The difference is in degree, not in character.

After a brief summary of two-dimensional separation symptoms (Section 1), various existing three-dimensional separation criteria are discussin (Section 2). Surface-flow visualizations and limited calculated results tend to support the envelope definition of separation, but additional descriptions are needed to determine separation correctly. Our open-vs-closed separation concept is elaborated in detail. Evidence of open separation reported during the last few years is presented in Section 3.

Separation patterns over typical bodies (ellipsoid of revolution, sharp and blunt cones, hemispherical cylinder, space shuttle orbiter) are discussed in Section 3. A more complete sequence of separation has recently been recognized and fits well with fragmentary experimental observations. In the last few years, a separation cycle from closed separation at low incidence to open separation at moderate incidence and to closed separation again at very high incidence has been developed.

The new elements are concerned with the transition steps from closed to open and from open to closed. Part of the separation sequence is found to be applicable to other geometries such as blunt cones and hemisphere cylinders.

In Section 4, separation patterns over airplane wings (infinite yawed wing, finite swept wing, transonic swept wing, delta wing) are examined. The wing flow exhibits a greater variety of separation patterns. At low incidence, separation on a finite swept wing of moderate to high aspect-ratio follows closely that over an infinite yawed wing, except near the tip where a tip vortex dominates. At high incidence the flow over the whole upper surface is separated, typically resulting in a spiral-vortex pattern, a part-span vortex spiral downstream above the wing's surface. A transonic swept wing is characterized by the presence of shocks and the shock-boundary layer interactions. The delta wing is best known for its leading-edge separation. Less known is the case without leading-edge separation which turns out to be just as interesting.

Surface flow patterns around various corners associated with protuberances (cylinder plate, fin-plate, flap-plate, cone-flare) are considered. The corner flow is characterized by horseshoe vortices, but is rather independent of protuberance geometry. The cylinder-plate case can be used as a model to bring out the essential features. Typically for a long cylinder, the flow separates ahead of the cylinder, followed by a reversed flow region. Above the plate, such reversed flow forms a horseshoe vortex which spirals away from the symmetry-plane down-

stream. The separated flow reattaches to the plate near the root of the cylinder. There, a counter-rotating vortex is formed, also extending downstream as a horseshoe vortex. If the height of the cylinder is decreased to be comparable with the plate' s boundary-layer thickness, the number of horseshoe vortex increases.

ACKNOWLEDGEMENT

The author is grateful to Dr. T. Hsieh of ARO Inc., Mr. K. F. Stetson of ARL, Dr. H. Werle of ONERA, and Prof. V. Zakkay of NYU for providing a number of photographs used in this work; and to Dr. S. H. Maslen of our Laboratories and Prof. M. V. Morkovin of IIT for their discussions. Thanks are also due to Prof. V. C, Patel of the University of Iowa and to Lockheed-Georgia Company for their invitation to the Viscous Flow Symposium at which this work was first presented.

7. REFERENCES

1. Maskell, E. C., "Flow Separation in Three Dimensions," RAE Report Aero 2565, Nov. 1955, Royal Aircraft Establishment, Bedford, England.

2. Peake, D. J., Rainbird, W. J., and Atraghji, E. G., "Three-Dimensional Flow Separations on Aircraft and Missiles," AIAA Journal, Vol. 10, No. 5, May 1972, pp. 567-580.

3. Korkegi, R. H., "Survey of Viscous Interactions Associated with High Mach Number Flight," AIAA Journal, Vol. 9, No. 5, May 1971, pp. 771-784.

4. Smith, J.H.R., "A Review of Separation in Steady, Three-Dimensional Flow," AGARD-CP-No. 168 on Flow Separation, Nov. 1975.

5. Brown, S. N. and Stewartson, "Laminar Separation", in Annual Review of Fluid Mechanics, Vol. 1, Annual Reviews Inc., Palo Alto, 1969.

6. Schlichting, H., Boundary Layer Theory, 6th Ed., McGraw-Hill, 1968.

7. Rosenhead, L. (Ed.), Laminar Boundary Layers, Oxford University Press, 1963.

8. Lighthill, M. J., Laminar Boundary Layers, Edited by L. Rosenhead, Oxford University Press, Oxford, England, 1963.

9. Kaplan, W., Ordinary Differential Equations, Addison-Wesley, Reading, Mass. 1958, Chapter 11.

10. Minorsky, N., Introduction to Nonlinear Mechanics, J.W. Edwards, 1947, Ann Arbor, Michigan.

11. Hayes, W. D., "The Three-Dimensional Boundary Layer," NAVORD Report 1313, May 1951, Naval Ordnance Research Lab., China Lake, California.

12. Moore, F. K., "Three-Dimensional Boundary Layer Theory," in Advances in Applied Mechanics, Vol. IV, Academic Press, N.Y., 1956.

13. Eichelbrenner, E. A. and Oudart, A., "Methode de Calcul de la Couche Limite Tridimensionnelle. Application a un Corps Fusele Incline sur le Vent," ONERA Publication 76, 1955, Paris, France.

14. Eichelbrenner, E. A., "Three-Dimensional Boundary Layers," in Annual Review of Fluid Mechanics, Vol. 5, 1973. Annual Review Inc., Palo Alto, California.

15. Stewartson, K., The Theory of Laminar Boundary Layers in Compressible Flows. Oxford University Press, 1964. Oxford, England.

16. Wang, K. C., "Separation Patterns of Boundary Layer Over an Inclined Body of Revolution," AIAA Journal, Vol. 10, No. 8, August 1972, pp. 1044-1050.

17. Wang, K. C. "Boundary Layer over a Blunt Body at High Incidence with an Open-Type of Separation," Proc. Royal Society, London, A. 340, pp. 33-55, 1974.

18. Wang, K. C., "Three-Dimensional Boundary Layer Near the Plane of Symmetry of a Spheroid at Incidence," Journal Fluid Mechanics, Vol. 43, 1, 187-209, 1970.

19. Wang, K. C., "Laminar Boundary Layer Near the Symmetry-Plane of a Prolate Spheroid," AIAA, Vol. 12, No. 7, 949-958, 1974.

20. Raetz, G. S., "A Method of Calculating Three-Dimensional Laminar Boundary Layers of Steady Compressible Flows," Report No. NAI 58-73, Northrop Corporation, December 1957.

21. Wang, K. C., "On the Determination of the Zones of Influence and Dependence for Three-Dimensional Boundary-Layer Equations," Journal of Fluid Mechanics, Vol. 48, Part 2, pp. 397-404, 1971.

22. Dwyer, H. A., "Boundary Layer on a Hypersonic Sharp Cone at Small Angle of Attack," AIAA Journal, Vol. 9, No. 2, Feb. 1971, pp. 277-284.

23. Boericke, R. R., "Laminar Boundary Layer on a Cone at Incidence in Supersonic Flow," AIAA Journal, Vol. 9, No. 3, March 1971, pp. 462-468.

24. McGowan III, J. J. and Davis, R. T., "Development of a Numerical Method to Solve the Three-Dimensional Compressible Laminar Boundary Layer Equations with Application to Elliptical Cones at Angle of Attack," ARL 70-0341, December 1970, Wright-Patterson Air Force Base, Ohio.

25. Lin, T. C. and Rubin, S. G., "Viscous Flow Over a Cone at Moderate Incidence. Part 2: Supersonic Boundary Layer," J. Fluid Mech. 59, 3, 1973, pp. 593-620.

26. Wang, K. C., "Boundary Layer over a Blunt Body at Extremely High Incidence," The Physics of Fluids, 17, 7, 1381-1385, 1974.

27. Wang, K. C., "Boundary Layer over a Blunt Body at Low Incidence with Circumferential Reversed Flow," Journal of Fluid Mechanics, 72, 1, 49-65, 1975.

28. Hsieh, T. and Wang, K. C. "Concentrated Vortex on the Nose of an Inclined Body of Revolution," Vol. 14, No. 5, 698-700, 1976.

29. Geissler, W., "Calculation of the Three-Dimensional Laminar Boundary Layer around Bodies of Revolution at Incidence and with Separation," in AGARD-CP-168, November 1975.

30. Eichelbrenner, E.A., "Decollement Laminaire en Trois Dimensions sur un Obstacle Fini," ONERA Publication No. 89, 1957.

31. Werle, H., "Separation on Axisymmetrical Bodies at Low Speed," La Recherche Aeronautique, No. 90, Sept.-Oct. 1962, pp. 3-14.

32. Stetson, K. F., "Boundary Layer Separation over Slender Cones at Angle of Attack," AIAA Journal, Vol. 10, No. 5, 1972, pp. 642-648.

33. Stetson, K. F., "Experimental Results of Laminar Boundary Layer Separation on a Slender Cone at Angle of Attack at M = 14.2," ARL 71-0127, August 1971, Aerospace Research Laboratories, Wright-Patterson.

34. Zakkay, V., Miyazawa, M. and Wang, C. R., "Lee Surface Flow Phenomena Over Space Shuttle at Large Angles of Attack at $M_\infty = 6$," NASA CR-132501, 1974; also AIAA Paper 75-148, January 1975.

35. Lubard, S. C., "Laminar Separation Over a Blunted Cone at High Angle of Attack," in AGARD-CP-168, November 1968.

36. Hsieh, T., "An Investigation of Separated Flow About a Hemisphere-Cylinder at Zero to 19 Deg. Incidences in the Mach Number Range from 0.6 to 1.5," to be published as AEDC-TR, Arnolds Research Organization, Inc.

37. Wild, J. M., "The Boundary Layer of Yawed Infinite Wings," Journal of the Aeronautical Sciences, Jan. 1949, pp. 41-45.

38. Monnerie, B., "Flow Field Aspects of Transonic Phenomena," AGARD-AR-82 on the Effects of Buffeting and Other Transonic Phenomena on Manuuvering Combat Aircraft, July 1975.

39. Vanino, R. and Wedemeyer, E., "Wind Tunnel Investigation of Buffet Loads on Four Airplane Models," AGARD-CP-87-71, 1971.

40. Kuchemann, D., "Types of Flow on Swept Wings," Journal of Royal Aero. Soc., Vol. 57, pp. 683-699, Nov. 1953.

41. Cooke, J. C. and Brebner, G. G., "The Nature of Separation and Its Prevention by Geometric Design in a Wholly Subsonic Flow," in Boundary Layer and Flow Control, Vol. 2, G. V. Lachman (Ed.), Pergamon Press, New York 1961.

42. Smith, A.M.O., "Remarks on Fluid Mechanics of the Stall," in AGARD-LS-74 on Aircraft Stalling and Buffeting, February, 1975.

43. Monnerie, B., "Decollement et Excitation Aerodynamiques Aux Vitesses Transsoniques," AGARD-LS-74 on Aircraft Stalling and Buffeting, February 1975.

44. Marsden, D. J., Simpson, R. W., and Rainbird, W. J., "The Flow Over Delta Wings at Low Speeds with Leading Edge Separation," CoA Report 114, Feb. 1958, The College of Aeronautics, Cranfield, England.

45. Werle, H., "Ecoulements Decolles Etude Phenomenologique a Partir De Visualisations Hydrodynamiques," AGARD-CP-168 on Flow Separation, Nov. 1975.

46. Carrier, G. F., "The Boundary Layer in a Corner," Quart. Applied Math. 4, pp. 367-370, 1946.

47. Rubin, S. G., "Incompressible Flow Along a Corner," Journal of Fluid Mechanics, Vol. 26, pt. 1, pp. 97-110, 1966.

48. Sedney, R., "A Survey of the Effects of Small Protuberances on Boundary-Layer Flows," AIAA Journal, Vol. 11, No. 6, June 1973, 782-792.

49. Ryan, B. M., "Summary of the Aerothermodynamic Interference Literature," Technical Note 4061-160, April 1969. Naval Weapons Center, China Lake, California.

50. Burbank, P. B., Newlander, R. A., and Collins, I. K., "Heat-Transfer and Pressure Measurements on a Flat-Plate Surface and Heat-Transfer Measurements on Attached Protuberances in a Supersonic Turbulent Boundary Layer at Mach Numbers of 2.65, 3.51, and 4.44," NASA TN D-1372, Dec. 1962.

51. Voitenko, D. M., Zubkov, A. I. and Panov, Yu, A., "Supersonic Gas Flow Past a Cylindrical Protuberance on a Plate, "Academy of Science Bulletin, USSR, Fluid and Gas Mechanics, No. 1, 1966, pp. 121-125; JHU/APL Translation TG 230-T515, Jan. 1967, Johns Hopkins University.

52. Thwaites, B., Incompressible Aerodynamics, Oxford University Press, 1960.

53. Rainbird, W. J., Crabbe, R. S., Peake, D. J. and Meyer, R. F., "Some Examples of Separation in Three-Dimensional Flow," Canadian Aero and Space Journal, Vol. 12, No. 10, December 1966.

54. Sedney, R. and Kitchens, C.W., Jr.: "The Structure of Three-Dimensional Separation Flows in Obstacle, Boundary-Layer Interactions," in AGARD-CP-168 on Flow Separation, Nov. 1975.

55. Young, F. L., Kaufman, L. G., and Korkegi, R.H., "Experimental Investigation of Interactions between Blunt Fin Shock Waves and Adjacent Boundary Layers at Mach Numbers 3 and 5, " ARL 68-0214, Dec. 1968, Aerospace Research Labs., Wright-Patterson.

56. Thomas, J. P., "Flow Investigation About a Fin Plate Model at a Mach Number of 11.26," ARL 67-0188, Sept. 1967, Aerospace Research Labs.

57. Bertram, M. H. and Henderson, A., Jr., "Some Recent Research with Viscous Interacting Flow in Hypersonic Streams," in Proceedings of 1969 Symposium, Viscous Interaction Phenomena in Supersonic and Hypersonic Flow, Aerospace Research Labs, Wright-Patterson.

58. Charwat, A. F. and Redekopp, L. G., "Supersonic Interference Flow Along the Corner of Intersecting Wedges," AIAA Journal, Vol. 5, No. 3, pp. 480-488, March 1967.

59. Watson, R. D. and Weinstein, L. M., "A Study of Hypersonic Corner Flow Interactions," AIAA Journal, Vol. 9, No. 7, July 1971, pp. 1280-1286.

60. Goldman, R. L. and Obremski, H. J., "Experimental Investigation of Hypersonic Buzz on a High Cross-Range Shuttle Configuration," NASA CR-112053, or RIAS TR 72-05C, May 1972. Also AIAA Journal, Vol. 11, No. 10, Oct. 1973, pp. 1361-1362.

61. Harris, J. E., "Aerodynamic Characteristics of a Series of Spherically Blunt 10^{o} Cones with 30^{o} and 60^{o} Base Flares," NASA TN D-3675, October 1966.